AN ABSTRACT OF THE THESIS OF

Michael Joseph Behrenfeld for the degree of Doctor of Philosophy in Oceanography presented on July 9, 1993.

Title: Effects of Ultraviolet-B Radiation on Marine Phytoplankton

Abstract approved: Redacted for privacy

Global increases in ultraviolet-B radiation (UVBR:290-320 nm) resulting from decreases in stratospheric ozone concentration have the potential to alter marine primary production and affect global climate and marine trophic dynamics. Effects of UVBR on phytoplankton carbon fixation were determined from open ocean exposure studies conducted off the coast of Washington state. Photoinhibition of carbon fixation was a linear function of cumulative UVBR dose weighted by an exponential action spectrum. Comparison of the dose-response for UVBR inhibition of carbon uptake with results of earlier research indicates that a common, short-term photoinhibition response to UVBR may occur.

Short-term photoinhibition was also measured for nitrogen uptake by natural plankton assemblages from the North Pacific. Ammonium uptake was inhibited by UVBR

exposure to a greater extent than nitrate uptake. The action spectrum for ammonium uptake inhibition had a lower slope and greater relative contribution from wavelengths >320 nm to total biologically effective dose than the action spectrum for total UVR (290-347 nm) inhibition of carbon fixation. Inhibition of ammonium uptake was a linear function of biologically effective UVR dose. Comparison between dose-responses and action spectra for ammonium and carbon uptake suggest deeper water-column penetration of UVR effects on ammonium uptake than carbon on uptake.

Influence of nutritional status on the photoinhibitory effects of UVBR on phytoplankton growth rates and biomass were investigated using monocultures of the marine diatom *Phaeodactylum tricornutum*. Specific growth rates and biomass were inhibited from 2% to 16% by UVBR during nutrient-replete growth. However, no effect of UVBR was detectable when inhibition of growth rate and biomass by nutrient limitation exceeded the potential for inhibition by UVBR. Thus, a competitive interaction appears to occur between macro-nutrient stress and UVBR stress, such that growth rate and biomass will be determined by the most limiting environmental factor. Results suggest that phytoplankton in nutrient-rich areas of the ocean may be most susceptible to UVBR inhibition of growth and biomass, while these parameters may not be appropriate for measuring UVBR stress in regions of nutrient limitation.

Effects of Ultraviolet-B Radiation on Marine Phytoplankton

by

Michael Joseph Behrenfeld

A THESIS

submitted to

Oregon State University

in partial fulfillment of

the requirements for the

degree of

Doctor of Philosophy

Completed July 9, 1993

Commencement June 1994

APPROVED:

Redacted for privacy

Professor in charge of major

Redacted for privacy

Head of Department of Oceanic and Atmospheric Sciences

Redacted for privacy

Dean of Graduate School

Date thesis is presented: July 9, 1993

Typed by Michael Behrenfeld

TABLE OF CONTENTS

LIST OF FIGURES

CONTRIBUTIONS OF AUTHORS

	Name	Contribution
Chapter 1:	John W. Chapman	Data analysis advice, technical assistance, cruise preparation and editorial comments on manuscript.
	John T. Hardy	Committee member: cruise preparation and editorial comments on manuscript.
	Henry Lee II	Committee member: program manager and editorial comments on manuscript.
Chapter 2:	David R.S. Lean	Analysis of ^{15}N samples using emissions spectrometer and editorial comments on manuscript.
	Henry Lee II	Committee member: program manager.
Chapter 3:	Henry Lee II	Committee member: program manager.
	Lawrence F. Small	Major professor: Data analysis advice, technical assistance, and editorial comments on manuscript.

EFFECTS OF ULTRAVIOLET-B RADIATION ON MARINE PHYTOPLANKTON

INTRODUCTION

The spectrum of solar electromagnetic radiation is altered by the earth's atmosphere before reaching the surface. Molecules in the atmosphere have specific absorption bands for electromagnetic radiation. Absorption of ultraviolet radiation (UVR) by oxygen and ozone are of particular interest. For meteorological purposes, the earth's atmosphere has been subdivided into various layers, the two layers closest to the surface being the troposphere (<13 km altitude) and the stratosphere (13 - 50 km alt.). Molecular oxygen (O_2) in the upper stratosphere effectively absorbs solar radiation <290 nm (i.e., ultraviolet-C radiation: UVCR). Absorption of UVCR less than 242.4 nm by O_2 results in dissociation into two singlet oxygen molecules (O) (Brasseur and De Rudder, 1983; McElroy and Salawitch, 1989). Singlet oxygen can re-associate with a molecule of O_2 to form a triatomic molecule of ozone (O_3). Ozone is destroyed by electromagnetic radiation with wavelengths greater than 220 nm, resulting in an equilibrium between stratospheric O_2 and O_3 (McElroy and Salawitch, 1989). Concentrations of atmospheric O_3 are greatest in the lower stratosphere, commonly referred to as the stratospheric ozone layer.

The ultraviolet absorption band of O_3 includes wavelengths of both UVCR and ultraviolet-B radiation (UVBR: 290-320 nm) (Brasseur and De Rudder, 1983). The stratospheric ozone layer increases the range of ultraviolet wavelengths absorbed by the atmosphere and the rate of atmospheric ultraviolet attenuation. Together, O_2 and O_3 attenuate all of the solar UVCR before reaching the earth's surface. Solar UVBR, however, is only partially attenuated by O_3 before reaching the surface. The intensity of UVBR at any particular location on the earth's surface is dependent upon ozone column thickness, latitude, time of day, season, and atmospheric conditions in the troposphere (primarily cloud density and urban tropospheric ozone concentration).

Dependence of atmospheric UVBR attenuation on ozone column thickness implies that changes in stratospheric ozone concentration would result in changes in surface UVBR intensity. Concern arose in the early 1970s that human activities may cause the reduction of stratospheric ozone concentration and a concomitant increase in biologically damaging UVBR. In 1974, Molina and Roland reported that surface releases of chlorofluorocarbons (CFCs) were in sufficient quantity to cause a measurable decrease in stratospheric ozone. Other ozone destroying compounds have since been identified and include halons, methylchloroform, hydrogenated chlorofluorocarbons, carbon tetrachloride, and methane (Kruger et al., 1982; McElroy and Salawitch, 1989;

Manzer, 1990). Freons (CFCs), however, are quantitatively the most important chemicals which threaten the stratospheric ozone layer, particularly Freon-11 ($CFCl_3$) and Freon-12 (CF_2Cl_3) (Manzer, 1990; Anderson et al., 1991). Anthropogenic pollutants which threaten the stratospheric ozone layer are inert chemicals with long atmospheric half-lives (Freon-11 and Freon-12 have the longest half-lives at 65 and 120 years, respectively) (Rodhe, 1990). Long atmospheric half-lives insure that stratospheric ozone depletion will continue well into the next century, even if international agreements such as the Montreal Protocol (Crawford, 1987) to halt production of ozone destroying chemicals are successful (McElroy and Salawitch, 1989; Watson et al., 1990).

Measurable decreases in stratospheric ozone concentration have already occurred (Brune et al., 1991; Stolarski et al., 1991; Frederick, 1993). Decreases in stratospheric ozone are greatest at high latitudes and negligible near the equator (Frederick, 1993), due to factors such as atmospheric circulation patterns and latitudinal variability in annual ozone production cycles. Rates of ozone depletion also show seasonal variability (Frederick, 1993). Currently, the annual rate of stratospheric ozone depletion is approximately 0.32-0.55% yr^{-1} between 30°-70°N latitude and 0.14-0.85% yr^{-1} between 30°-60°S latitude (Stolarski et al., 1991; Stolarski et al.,

1992; Frederick, 1993). Largest decreases in stratospheric ozone have occurred each austral spring over Antarctica since 1978 (the "Antarctic ozone hole"), exceeding 50% depletion during recent years compared to 1977 levels (Kerr, 1989; Yung et al., 1990, Anderson et al., 1991; Schoeberl and Hartmann, 1991).

Decreases in stratospheric ozone concentration are expected to result in increased surface UVBR intensities. Conclusive evidence of increased UVBR from ground-based measurements has only been collected in Antarctica during the "Antarctic ozone hole" events (Frederick and Snell, 1988; Lubin et al., 1989). Indecisive evidence of increased UVBR outside of the Antarctic region is likely due to the lack of a global UVBR monitoring program, a deficiency in the number and quality of historical UVBR measurements with which to compare current UVBR measurements, and difficulty in deciphering between natural variability in UVBR intensity and the relatively small signal of a UVBR increase (Frederick, 1993). Reliance upon radiative transfer models for estimating the effects of current and future decreases in stratospheric ozone on surface UVBR intensities has resulted from the difficulty associated with making accurate ground-based measurements of increased UVBR. The radiative transfer model of Green et al. (1980) indicates the largest increases in UVBR energy from ozone depletion will occur at wavelengths between 310-320 nm, while the largest relative

increases will occur at wavelengths <310 nm. Other models suggest similar spectral effects of ozone depletion on surface UVBR, but often differ with respect to the absolute increase in UVBR energy (Frederick and Lubin, 1988).

Increases in surface UVBR may have important implications on individual organisms or biological communities. Ultraviolet-B radiation causes death in microorganisms (Fisher and McKinley, 1927; Harm, 1980; Rambler and Marguilis, 1980; Jagger, 1981), damages cell membranes (Mantai et al., 1970; Moss and Smith, 1981; Murphy, 1983), induces lesions in genetic material which can result in phenotypic mutations (Lyman et al., 1961; Harm, 1980; Karantz et al., 1991), and decreases photosynthesis, growth, and pigment concentration in vascular plants (Teramura, 1980; Trocine et al., 1981; Caldwell et al., 1983; Wellmann et al., 1984; Kulandaivelu et al., 1989; Strid et al., 1990) and in non-vascular plants (Platt et al., 1980; Smith and Baker, 1980; Worrest, 1983; Jokiel and York, 1984; Maske, 1984; Wood, 1987; Lesser and Shick, 1989; Behrenfeld et al. 1992).

Aquatic organisms are not completely protected from the effects of solar UVBR by their aqueous environment. The possible biological importance of UVBR in the surface ocean was first recognized by Jerlov (1950). Although attenuation of UVBR is rapid compared to most wavelengths of photosynthetically active radiation (PAR: 400-700 nm), 1% of

surface UVBR may reach depths of nearly 30 m in the clearest ocean waters (Smith and Baker, 1981). Phytoplankton are particularly susceptible to the adverse effects of increased UVBR because they are single celled organisms which are obligated to the surface euphotic zone, a portion of which is illuminated by UVBR. Changes in phytoplankton biomass by increases in UVBR could have implications for higher trophic levels because phytoplankton form the base of the marine food web (Hardy and Gucinski, 1989), or such changes could influence global climate by changing the oceans' capacity for atmospheric CO_2 uptake or release of dimethyl sulfide (Sigleo and Behrenfeld, 1992).

Study of photoinhibition by UVBR in natural marine phytoplankton assemblages has been limited primarily to short-term experiments involving radiolabeled carbon uptake by the phytoplankton. Lorenzen (1979) measured in-situ photosynthetic carbon uptake by coastal phytoplankton in UVBR-transparent and UVBR-opaque vessels and reported detectable inhibition of carbon uptake by ambient UVBR in the upper 1.2 - 1.5 m, corresponding to 0.1 - 0.01% of the surface UVBR intensity. Additional measurements of decreased carbon uptake by ambient UVR indicate that both UVBR and ultraviolet-A radiation (UVAR: 320-400 nm) inhibit photosynthesis in the upper euphotic zone (Worrest et al., 1980; Hobson and Hartley, 1983; Maske, 1984; Bühlmann et al., 1987; Helbling et al., 1992; Smith et al., 1992).

Paerl et al. (1985) reported significant decreases in photosynthetic carbon uptake by eucaryotic phytoplankton, and complete tolerance to surface intensities of UVBR in the cyanobacterium *Microcystis aeruginosa*. Short-term photoinhibition by UVBR has also been measured during laboratory studies on phytoplankton monocultures. Döhler et al. (1987) found that both short-term carbon uptake and ammonium assimilation by the marine diatom *Lithodesmium variabile* were sensitive to UVBR exposure. McLeod and Kanwisher (1962) reported a decrease in the quantum efficiency of photosynthetic oxygen evolution in monocultures of *Phaeodactylum tricornutum* and *Dunaliella tertecolata*, after UVR exposure. Oxygen evolution from the Hill reaction is photoinhibited by ultraviolet wavelengths <350 nm (Mantai et al., 1970; Hirosawa and Miyanhi, 1983), but can be photoreactivated by UVAR and PAR wavelengths (Van Baalen and O'Donnell 1972; Hirosawa and Miyanhi, 1983).

Measurements of in-situ photoinhibition by ambient intensities of solar UVBR provide evidence that surface phytoplankton are currently inhibited by UVBR. However, estimates of photoinhibition from enhanced UVBR based on ambient UVBR effects measurements require extrapolation of dose-responses beyond the range of UVBR used during these studies. On the other hand, laboratory studies of UVBR effects on marine phytoplankton provide insight toward the physiological effects of UVBR, but are difficult to equate

to natural phytoplankton populations. Ideally, estimates of the effects of increased surface UVBR on phytoplankton productivity should be based on experimental data collected using natural phytoplankton assemblages and UVBR doses which include and exceed those expected to occur with stratospheric ozone depletion. Exposure studies using UVBR intensities enhanced above ambient require the use of an artificial ultraviolet source. Measurements of photoinhibition by ambient UVBR and enhanced UVBR should be included in such studies in order to identify any effects of spectral differences between solar and lamp UVBR radiation.

Smith et al. (1980) completed the first ambient and enhanced UVBR effects study using natural phytoplankton assemblages collected from various oceanic regions. Photoinhibition by UVBR was determined from differences in radiolabeled carbon uptake between UVBR treatments. Some of the enhanced UVR treatments included both UVBR and UVCR. Smith et al. (1980) found an increase in the damaging efficiency of UVR with decreasing wavelength. Wavelength dependence of a physiological response requires application of amplification factors (i.e., an action spectrum) for calculation of the biologically effective dose required for response comparisons between spectrally distinct UVR treatments. Smith et al. (1980) compared dose-responses for inhibition of phytoplankton carbon uptake measured in the various UVR treatments by weighting UVR dose with previously

described action spectra determined from dissimilar biological processes. Action spectra used for the comparison were 1) the photoinhibition action spectrum of Jones and Kok (1966), derived from Hill reaction inhibition of spinach chloroplasts, 2) the Caldwell (1971) plant action spectrum, derived from the damage spectra of several terrestrial plants, and 3) the DNA action spectrum of Setlow (1974), derived from photoproducts in DNA and the mutation rates and mortality of bacteria and phages. Smith et al. (1980) found inhibition of phytoplankton carbon fixation by UVR to be a linear function of cumulative dose when the UVR dose was weighted by the photoinhibition action spectrum of Jones and Kok (1966).

Results of the study by Smith et al. (1980) were an important advancement in the understanding of UVBR effects on marine phytoplankton. However, their dose-response model for photoinhibition by UVBR could be improved by utilizing an action spectrum specific for UVBR inhibition of the metabolic process being measured (not of the Hill reaction used by Jones and Kok, 1966), by expanding the geographical distribution of UVBR effects measurements, and by using enhanced UVR treatments that do not include UVCR wavelengths (since UVCR is completely absorbed by the atmosphere before reaching the surface). Models of UVBR effects on phytoplankton would also be improved by including dose-

response relationships based on metabolic processes other than carbon uptake.

Measurements of photoinhibition by UVBR on short-term processes (e.g., carbon fixation) during open ocean studies on natural phytoplankton assemblages are beneficial because they avoid, to a large extent, experimental artifacts such as species changes and nutrient depletion which occur during longer-term, closed bottle growth studies. However, it is not clear whether dose-response models based on short-term exposures are indicative of the longer-term effects of UVBR on phytoplankton growth rates and biomass.

Measurements of the long-term inhibitory effects of UVBR on phytoplankton growth and biomass have been limited almost entirely to laboratory studies using phytoplankton monocultures. Jokiel and York (1984) reported decreased growth rates by UVBR in *Symbiodinium microadriaticum* (symbionic dinoflagellate), *Phaeodactylum tricornutum* (diatom), and *Oscillatoria lud* (filamentous cyanobacterium), but not in *Chaetoceros gracilis* (diatom), *Tetraselmis sp.* (green alga), or *Isochrysis sp.* (tropical flagellate). Similarly, Calkins and Thordardottir (1980) found a range of UVBR sensitivities within diatom species collected from Iceland. During their study, *Chaetoceros debilis*, *Chaetoceros decipiens*, *Skeletonema sp.*, and *Nitzschia sp.* exhibited UVBR sensitivity, while *Thalassiosira gravida* was UVBR tolerant and *Thalassiosira polychorda* had an apparent

threshold for UVBR inhibition. Species-specific effects of UVBR on growth and biomass have also been reported for other phytoplankton monocultures (Thomson et al., 1980; Wolniakowski, 1980; Worrest et al., 1981a; Döhler, 1984a; Döhler, 1984b; Döhler et al., 1987; Ekelund, 1990; Behrenfeld et al., 1992). A limited number of long-term UVBR effects studies have been completed using natural phytoplankton populations (Bidigare, 1989; El-Sayed et al., 1990; Helbling et al., 1992; Bothwell et al., 1993) or microcosms (Worrest et al., 1978; Worrest et al., 1981b). Effects of UVBR measured during these studies included changes in pigment concentration (Bidigare, 1989; El-Sayed et al., 1990; Helbling et al., 1992) and species composition (Worrest et al., 1978; Worrest et al., 1981b; Helbling et al., 1992; Bothwell et al., 1993).

A characteristic common to all previous studies of UVBR effects on phytoplankton growth and biomass has been the use of culture medium which is either naturally enriched or artificially enriched in nutrients (i.e., nutrient-replete). Effects of UVBR on nutrient-replete phytoplankton may, at best, simulate effects in oceanic regions with similar nutrient conditions, such as during the onset of the coastal spring blooms at mid-latitudes. Nutrient concentrations in most oceanic regions, however, are far from replete. Studies of UVBR effects utilizing low nutrient concentrations or nutrient-limited cultures are needed to

assess the possible effects of increased UVBR on growth and biomass of phytoplankton in low-nutrient regions of the ocean.

Objectives of my research were to 1) describe an action spectrum for photoinhibition of carbon fixation using natural assemblages of marine phytoplankton, 2) determine the dose-response relationship between phytoplankton carbon fixation and UVBR dose weighted by the new action spectrum, 3) describe the action spectrum and dose-response of UVBR inhibition of natural marine phytoplankton based upon a metabolic process other than carbon fixation, and 4) describe the relationship between macro-nutrient status and UVBR stress on the growth rate and biomass of a marine phytoplankton species.

The action spectrum and dose-response for UVBR inhibition of phytoplankton carbon uptake were determined during UVBR exposure experiments conducted during a cruise off the Washington state coast (Chapter 1). Results of this research are compared to the earlier study by Smith et al. (1980). Studies on the effects of UVBR on a metabolic process of phytoplankton other than carbon uptake were completed during a cruise in the North Pacific ocean using measurements of [^{15}N]nitrate and [^{15}N]ammonium uptake (Chapter 2). A dose-response and action spectrum for ammonium uptake inhibition was determined and compared to the dose-response and action spectrum for UVBR inhibition of

carbon uptake. Finally, the influence of nutritional status on the photoinhibitory potential of UVBR on phytoplankton growth rate and biomass was measured using nutrient-replete and macro-nutrient-limited cultures of the marine diatom *Phaeodactylum tricornutum* (Chapter 3).

CHAPTER 1: IS THERE A COMMON RESPONSE TO ULTRAVIOLET-B RADIATION BY MARINE PHYTOPLANKTON?

by: Michael J. Behrenfeld, John W. Chapman, John T. Hardy, and Henry Lee II

ABSTRACT

Global increases in ultraviolet-B radiation (UVBR) have the potential to alter marine primary production and affect carbon cycles and marine trophic dynamics. Estimates of UVBR induced photoinhibition have varied greatly, indicating that a common dose response by marine phytoplankton may not occur. A linear, wavelength specific response of phytoplankton to both natural and artificial sources of UVBR was discovered with the application of a simple exponential action spectrum. Application of this new action spectrum to data presented here as well as data reported previously, indicates that a common, short-term photoinhibition response to UVBR may occur. The average photoinhibition of marine phytoplankton by UVBR appears to be a linear response to UVBR dose.

ACKNOWLEDGEMENTS

The authors thank the crew of the R.V. Discoverer and Chief Scientist Timothy Bates without whose help this research would not have been possible. We also thank Lawrence Small, Evelyn Sherr, and Earl Davey for helpful suggestions on the manuscript.

This research was funded by the USEPA under contract 68-CO-0051 and represents EPA:ERL-N contribution number N215.

INTRODUCTION

The quantitative effects of UV-B radiation (UVBR: 290-320 nm) on marine primary production have been the focus of intensive research almost since stratospheric ozone depletion was discovered (Lorenzen, 1979; Smith et al., 1980; Worrest et al., 1981a; Helbling et al., 1992; Smith et al., 1991; Behrenfeld et al., 1992; Behrenfeld et al., 1993). Developing a reliable estimate of the dose response of marine phytoplankton to UVBR has been a common goal of this research, yet has remained elusive largely due to an incomplete knowledge of wavelength dependent biological effects of UVBR.

Stratospheric ozone depletion will result in disproportionate increases in the 290-300 nm range of the UVBR spectrum relative to longer wavelengths (Green et al., 1980). Since shorter UVBR wavelengths cause more biological damage per unit of energy than longer UVBR wavelengths (Jones and Kok, 1966; Caldwell, 1971; Setlow, 1974), projected global increases in biologically harmful UVBR will be proportionately greater than total increases in UVBR energy. Biological effects of UVBR at each wavelength are extremely difficult to determine independently in nature. Action spectra, mathematical weighting functions, are therefore applied to irradiation doses from entire radiation spectra when estimates of biological effect are of interest.

Applications of action spectra are optimal when limited to the organisms (or cellular components) from which they are derived. However, experimental determinations of action spectra for every organism or cell component of interest is impractical. Therefore, action spectra are commonly applied to experimental irradiance conditions vastly different from the conditions in which they were originally determined.

The most commonly applied action spectra in studies of UVBR effects on marine phytoplankton were not derived for marine phytoplankton. These action spectra are: 1) the photoinhibition action spectrum (P.I.) of Jones and Kok (1966), derived from Hill reaction inhibition of spinach chloroplasts by radiation between 260 to > 560 nm; 2) the Caldwell plant action spectrum (CPA) (1971), derived from damage spectra of several terrestrial plants for wavelengths < 313 nm; and 3) the DNA action spectrum of Setlow (1974) derived from photoproducts in DNA and the mutation rates and mortality of bacteria and phages at wavelengths between 250 and 370 nm. Irradiance spectra used in these studies, and perhaps every subsequent study, have been measured using different methods. These differences in measurement techniques must result in systematic errors that are themselves a likely additional sources of error in estimates of damage. Action spectra should thus be applied to dose response data with caution.

The largest data sets available on photoinhibition (decrease in carbon fixation) by UVBR in natural marine phytoplankton are those of Smith et al. (1980) and Behrenfeld et al. (1993). Their results are dramatically different despite similar methods used to determine photoinhibition. Photoinhibition was described by Smith et al. (1980) as a linear function of UVBR doses weighted by the P.I. action spectrum. Behrenfeld et al. (1993) found the DNA action spectrum best described the wavelength specific photoinhibition by UVBR, even though the effect was probably not due to DNA damage. The DNA action spectrum gives shorter wavelengths a relatively greater effective weight than the P.I. action spectrum. This difference is critical since a 17.4% increase in mid-latitude noon UVBR from ozone depletion (Green et al., 1980; Stolarski et al., 1992) would correspond to an increase in biologically effective UVBR of only 20% when weighted by the P.I. action spectrum compared to an 85% increase when weighted by the DNA action spectrum.

In the current study, a biological action spectrum, consisting of a simple exponent, was derived from comparisons of phytoplankton to a diversity of spectral conditions and UVBR doses. Application of the exponential action spectrum to data from previous studies (Smith et al., 1980; Behrenfeld et al., 1993) indicates a common phytoplankton response to UVBR.

MATERIALS AND METHODS

UVBR exposure experiments were conducted during April, 1991 between 48°N, 125°W and 48°N, 128°W on board the NOAA R.V. Discoverer. Phytoplankton carbon fixation rates were determined using the carbon-14 light and dark bottle technique (Parsons et al., 1984). Phytoplankton samples were collected from the upper 2 m of the ocean surface. Samples were immediately dispensed into 250 ml UVBR transparent FEP Teflon^{R} bottles, inoculated with 10 µCi $NaH^{14}CO_3$, and incubated for 4-8 hr in an on-deck incubator (Behrenfeld et al., 1993). Flow-through seawater maintained the samples at sea surface temperatures during incubation. Five replicates were used in each of 4 treatments: 1) UVBR excluded, 2) ambient UVBR, 3) UVBR enhanced above ambient, and 4) dark. Following incubation, each sample was filtered through a 0.45 µm polycarbonate filter (Millipore^{R}) at 70 kPa. The filters were then fumed over concentrated HCl for 3 min to remove inorganic carbon. Carbon uptake rates (mg C m^{-3} h^{-1}) were determined by liquid scintillation counting. Counts per minute measured by the scintillation counter (Packard Model 2000CA) were corrected for background and quenching using a radioactive standard. Carbon-14 uptake in the dark treatment was subtracted from the light treatments.

Ultraviolet fluorescent lamps (UVB 313, Q-Panel Co.), pre-burned for approximately 100 hrs, were used to create the enhanced UVBR treatment. The lamps were located beneath an incubation tank with a UVBR transparent acrylic (Acrylite OP-4, CYRO Industries) bottom. A 0.13 mm sheet of cellulose acetate between the lamps and the enhanced UVBR treatment bottles eliminated lamp radiation <290 nm. A 0.13 mm sheet of Mylar^{R} between the lamps and all other bottles eliminated lamp radiation <315 nm. Bottles in the UVBR excluded treatment were wrapped with a 0.13 mm sheet of Mylar^{R} to eliminate all solar wavelengths <315 nm. Cellulose acetate and Mylar^{R} films were replaced periodically to avoid photodegradative changes in transmittance properties. Neutral density screen (gray plastic mesh) was used between the lamps and the incubation tank to adjust the intensity of the enhanced UVBR dose.

Ambient solar radiation (285-800 nm) was continuously monitored using an Optronic Model 752 spectroradiometer clear of all shading mounted on the uppermost deck of the ship. The spectroradiometer was calibrated for wavelength offset by scanning a mercury arc lamp and for intensity using a halogen lamp traceable to the National Institute of Standards and Technology. The Optronic 752 has a reported wavelength accuracy of ±0.3 nm, wavelength precision of ±0.1 nm, and an intensity accuracy of ±2-4% for the entire range of 200-800 nm. This spectroradiometer was also used to

measure the UVBR dose from the lamps beneath the incubation chamber.

RESULTS

Phytoplankton were sampled both inside and outside of the coastal upwelling region off the Washington state coast. Carbon fixation rates were high (12.1 - 39.2 mg C m^{-3} hr^{-1}) inside and low (0.3 - 0.9 mg C m^{-3} hr^{-1}) outside the upwelling region (Table 1). Compared to uptake in the ambient UVBR treatment, exclusion of solar UVBR resulted in enhanced carbon fixation rates, while enhancement of UVBR depressed carbon fixation (Table 1).

Comparisons of the percent decrease in carbon fixation per total unweighted UVBR dose between the ambient and excluded treatments and the ambient and enhanced treatments reveal separate, linear dose responses (Fig. 1-1a). Lamp radiation produced greater decreases in carbon fixation per unit UVBR energy than did solar radiation (Fig. 1-1a). The ultraviolet fluorescent lamps produce a spectrum more enriched in the short UVBR wavelengths compared to the solar spectrum (Fig. 1-2) and, therefore, a greater biologically effective dose per unit of energy. The lesser effect of solar UVBR compared to artificially enhanced UVBR (Fig. 1-1a) indicates, once again, that application of an action spectrum to the spectral data is necessary to compare dose responses of the different UVBR spectra.

The correct, or "best fit", action spectrum will result in convergence of the slopes and intercepts of dose

Table 1. Carbon fixation rates (mg C m^{-3} hr^{-1}) in the UVBR excluded, ambient UVBR, and enhanced UVBR treatments for each experiment. Standard deviations are indicated in brackets.

Date	Excluded	Ambient	Enhanced
04/18/91	0.6 (±0.04)	0.6 (±0.03)	0.4 (±0.04)
04/19/91	0.7 (±0.05)	0.7 (±0.03)	0.5 (±0.02)
04/20/91	0.7 (±0.02)	0.6 (±0.05)	0.5 (±0.04)
04/21/91	0.8 (±0.04)	0.6 (±0.08)	0.4 (±0.03)
04/22/91	16.7 (±0.93)	15.5 (±0.57)	13.4 (±1.26)
04/23/91	12.1 (±0.76)	12.4 (±0.69)	7.8 (±1.00)
04/24/91	20.4 (±1.22)	19.3 (±2.30)	16.4 (±0.22)
04/25/91	0.9 (±0.30)	0.9 (±0.11)	0.8 (±0.26)
04/26/91	0.7 (±0.16)	0.6 (±0.07)	0.4 (±0.05)
04/27/91	39.2 (±3.31)	30.7 (±0.76)	18.7 (±1.94)
04/28/91	35.3 (±4.25)	28.0 (±2.04)	22.1 (±4.36)

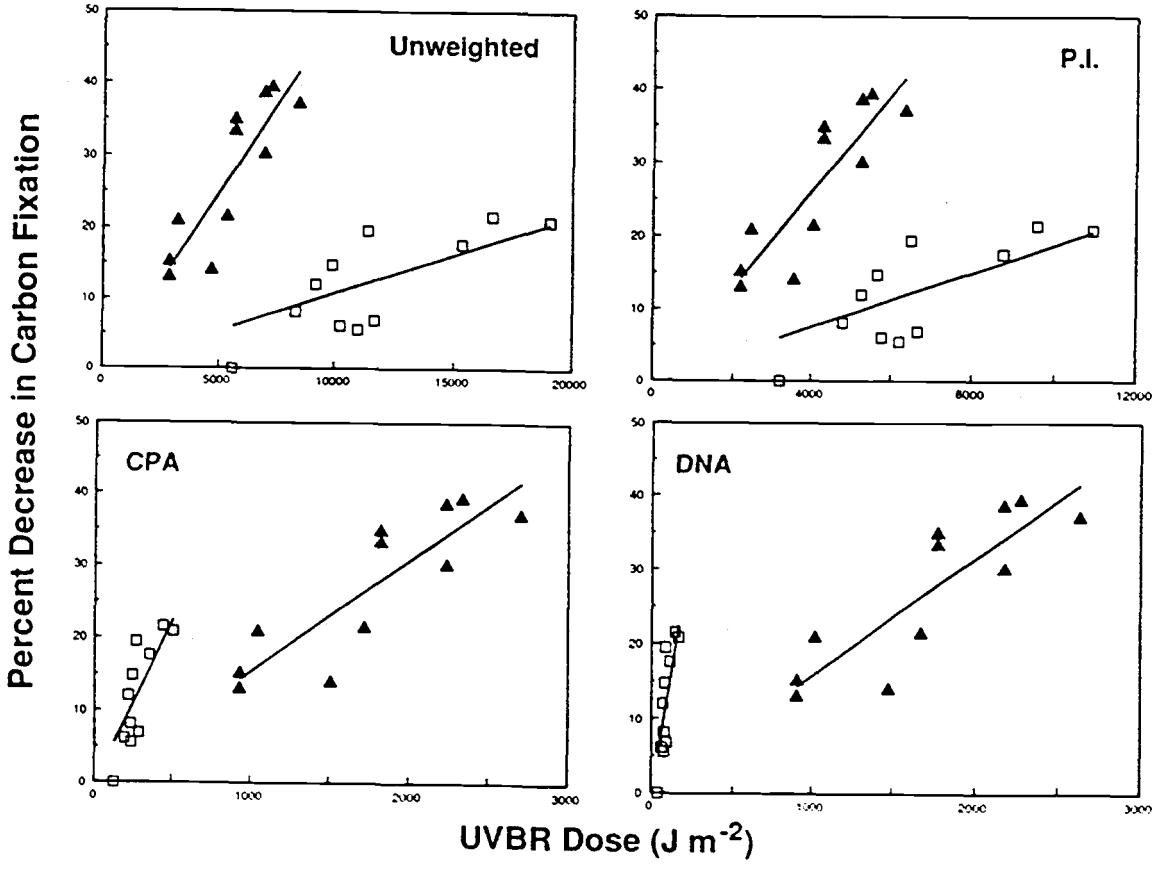

Figure 1-1. Percent decrease in carbon fixation as a function of UVBR dose. (A) unweighted UVBR doses, (B) UVBR weighted by the P.I. action spectrum of Jones and Kok, (C) UVBR doses weighted by the Caldwell plant action spectrum, and (D) doses weighted by the DNA action spectrum of Setlow. All action spectra are normalized to 1 at 300 nm. Decreases between the UVBR excluded and ambient UVBR treatments are indicated by □. Decreases between the ambient and enhanced UVBR treatments are indicated by ▲.

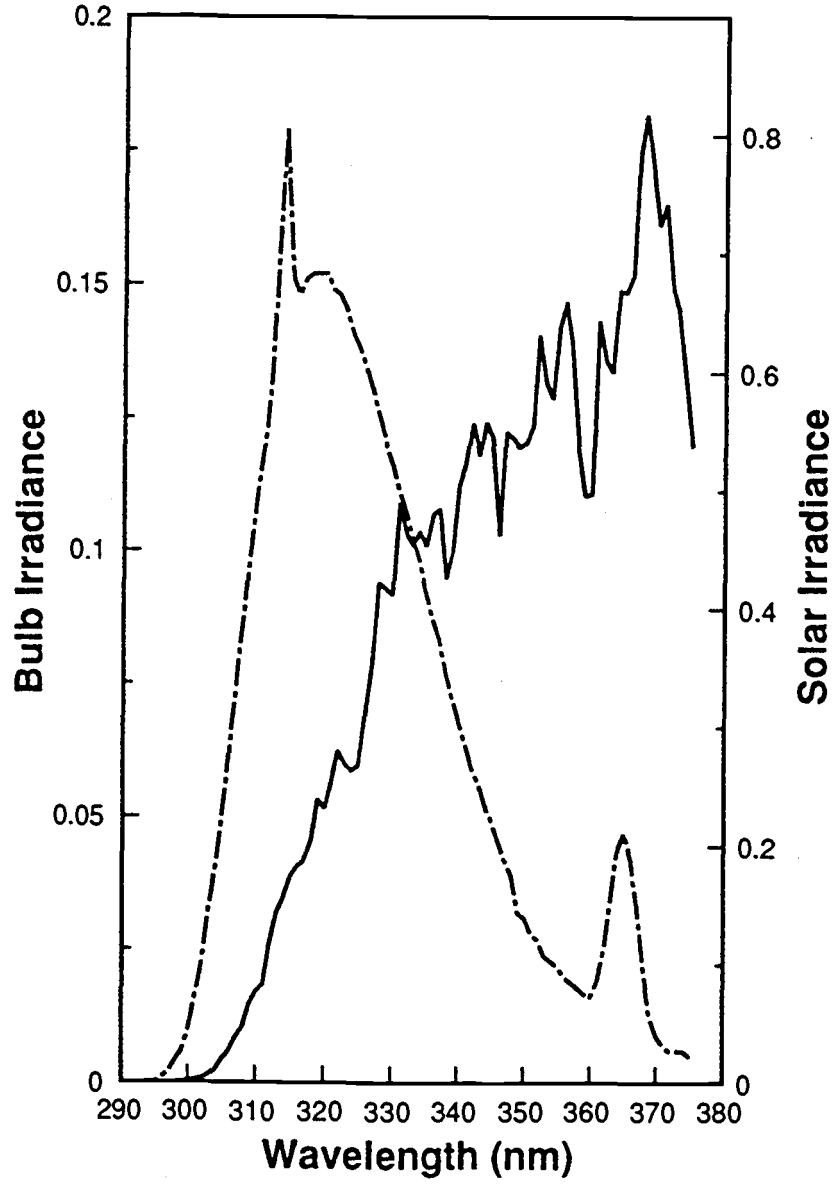

Figure 1-2. Spectral distribution and relative intensity of solar (45°N) (——) and lamp (–·–) radiation measured with an Optronic model 752 spectroradiometer.

responses calculated independently from divergent radiation spectra and the highest regression coefficient for the combined data. The P.I., CPA, and the DNA action spectra all give more biologically effective weight to short wavelengths than long wavelengths. Of the three action spectra, the P.I. spectrum has the least slope and the DNA spectrum has the greatest slope (Fig. 1-3a). None of these pre-determined action spectra satisfy the criterion for the "best fit" action spectrum (Fig. 1-1b,c,d), although the "best fit" action spectrum clearly lies between the P.I. and the DNA spectra.

Fortuitously, the P.I., CPA, and DNA action spectra are closely approximated between 290 and 320 nm by an exponential model:

$$\text{Action spectra} = \alpha e^{c\lambda} \qquad (1)$$

where; c is a constant describing the slope of the curve, λ is wavelength between 290 and 320 nm, and α is a normalization factor (Fig. 1-3a). An exponential action spectrum (where c=-0.022) describes the P.I. spectrum almost exactly. The DNA and CPA spectra deviate from an exponential model at the shortest and longest wavelengths, respectively (Fig. 1-3b).

The action spectrum for UVBR induced photoinhibition of phytoplankton carbon fixation can be determined from (eq. 1) by choosing a value for "c" which satisfies the "best fit"

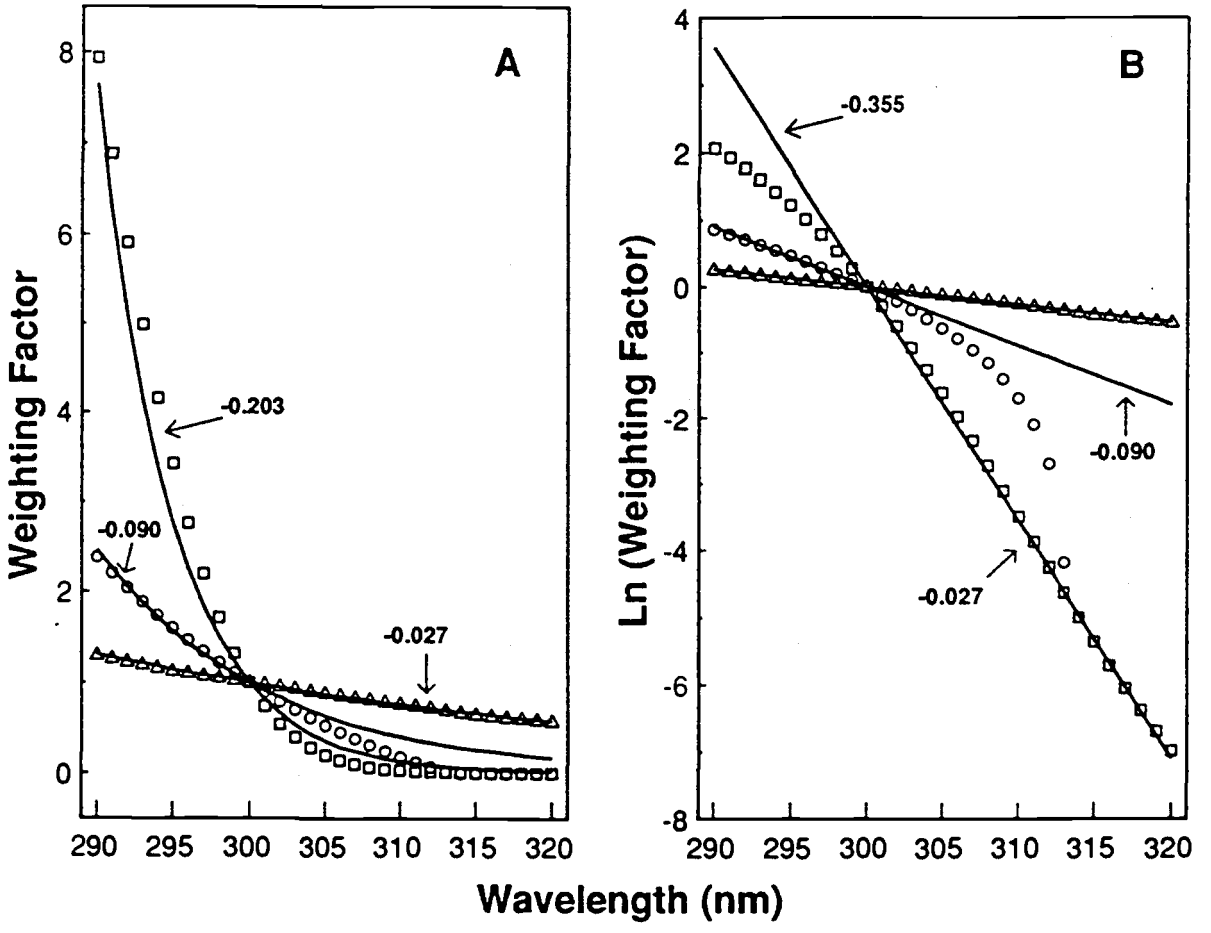

Figure 1-3. Comparison of P.I. (Δ), CPA (O), and DNA (□) action spectra with exponential curves (A) and expanded on a Ln:Normal scale to show the relationships more clearly (B). Exponent values are indicated for each curve. (A) DNA action spectrum compared to "best fit" exponential (-0.134; eq. 2) and (B) exponent derived from the linear portion of the ln transformed DNA action spectrum (-0.356). All action spectra normalized to 1 at 300 nm.

criterion. Advantages of such an action spectrum are its direct relevance to the cellular target(s) of interest and the fewer assumptions required for its application compared to more complex action spectra used previously. The best fit exponential action spectrum, normalized to 1 at 300 nm was:

$$\text{Action spectra} = 3.32*10^{17}\ e^{-0.134\lambda} \text{ (Fig. 1-4a)} \qquad (2)$$

The dose range can be expanded by comparing carbon fixation rates in the ambient and enhanced UVBR treatments to the UVBR excluded treatment (Fig. 1-4b), resulting in the dose response relationship:

$$P_C = 0.012\ Q_{EXP} \quad (R^2 = 0.86,\ p < 0.001,\ n = 22) \qquad (3)$$

where, P_C is the percent of photoinhibition calculated as $[(CF_{EXCL}-CF_{UVB})/CF_{EXCL}]*100$, CF_{EXCL} is carbon fixation in the UVBR excluded treatment, CF_{UVB} is carbon fixation in either the ambient or enhanced treatment, and Q_{EXP} is the total dose of UVBR (J m^{-2}) weighted by the "best fit" exponential action spectrum (eq. 2) normalized to 1 at 300 nm. The regression slope (eq. 3) is half as steep as the regression slope reported by Behrenfeld et al. (1993a) ($P_C = 0.022\ Q_{DNA}$), where cumulative UVBR dose (Q_{DNA}) was weighted by the DNA action spectrum normalized to 1 at 300 nm (i.e., DNA_{300}).

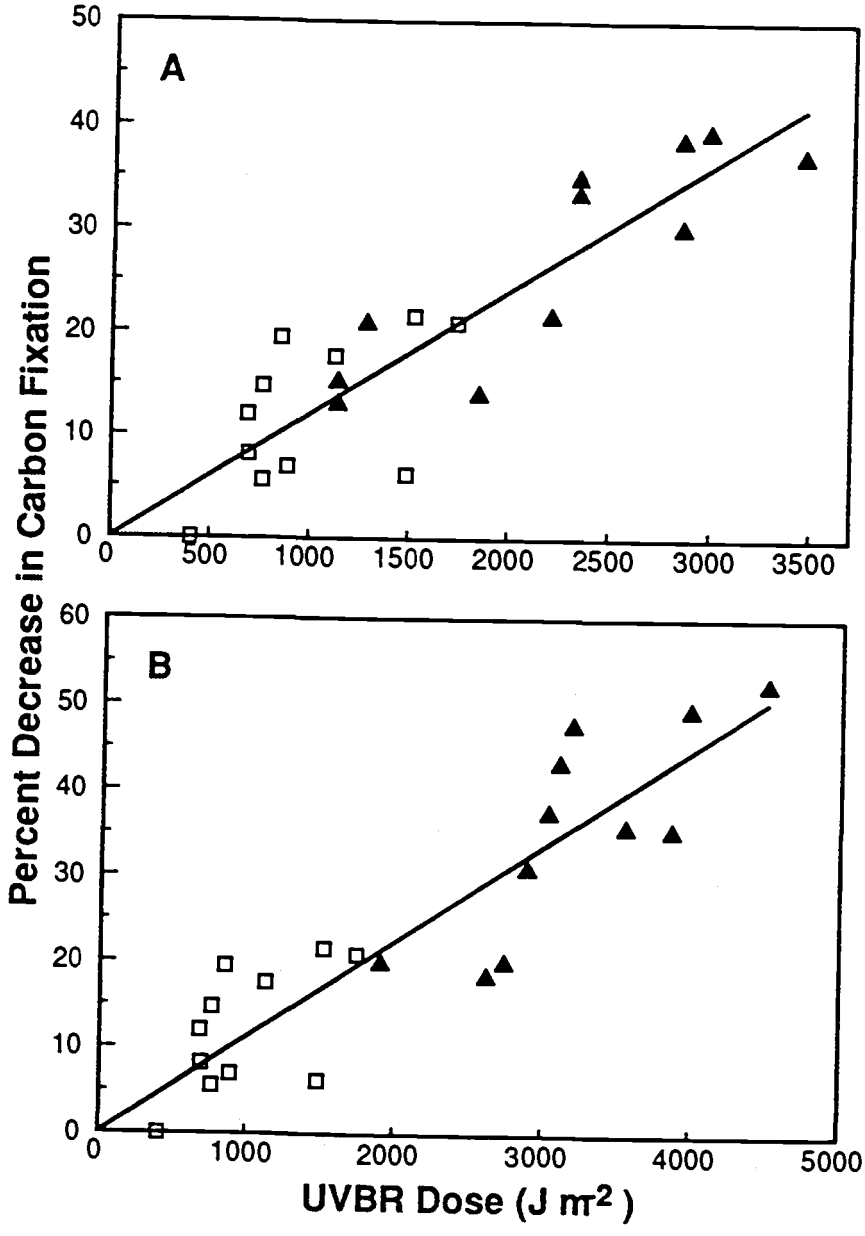

Figure 1-4. Dose response using the "best fit" exponential action spectrum (eq. 2). (A) Dose response for percent decrease in carbon fixation between ambient and excluded UVBR treatments and ambient and enhanced UVBR treatments (R^2=0.78). (B) Same dose response as in (A) except with the range of doses expanded by making all comparisons to the UVBR excluded treatment (R^2=0.86). □ = Effect of solar UVBR. ▲ = Effect of enhanced UVBR.

However, lower slope of the dose-response could have been anticipated since the "best fit" action spectrum (eq. 2) is approximately half as steep as the DNA action spectrum (Fig. 4a,b).

These results must be interpreted with caution. The experiments were of short duration and may not be representative of the longer term effects of UVBR on growth and biomass. Furthermore, these experiments were performed using closed bottles for 6 hrs which very likely create unnatural effects. Unfortunately, the closed bottle ^{14}C method will remain one of the most commonly used methods for studying open ocean phytoplankton production until practical alternatives are developed.

DISCUSSION

We found photoinhibition of carbon fixation by UVBR is a linear function of UVBR dose weighted by the "best fit" action spectrum (eq. 2). Dose responses reported from earlier studies vary from linear (Smith et al., 1980) to sigmoidal (Helbling et al., 1992) for biologically weighted and unweighted UVBR doses. Although a complete review of UVBR literature is beyond the scope of this report, we have made an intercomparison between our dose response and dose responses reported by Smith et al. (1980) and Behrenfeld et al. (1993). These two studies provided the largest data sets on UVBR induced inhibition of phytoplankton carbon fixation. When UVBR doses from these studies (Smith et al., 1980; Behrenfeld et al., 1993) are converted to UVBR doses weighted by our new exponential action spectra, nearly all the data converge upon a single, linear dose response.

The only response data which diverge from this general pattern is the "altered" treatment data from Smith et al. (1980). Comparisons between UVBR doses weighted by various action spectra indicate that this divergence probably results from limitations of the "best fit" action spectrum for non-UVBR wavelengths.

The "best fit" action spectrum results in a dose response with no apparent threshold. However, a threshold is apparent when the dose response to solar UVBR is

calculated using unweighted UVBR doses. Thus, sigmoidal dose responses recently reported for photoinhibition by UVBR may result simply because an action spectrum was not applied.

Intercomparison of Dose Responses

UVBR dose response data from two previous field studies (Behrenfeld et al., 1993), when recalculated using the new action spectrum (eq. 2), closely correspond with data herein and there appears to be no distinguishable threshold (Fig. 1-5). The dose response for the combined data is:

$$P_C = 0.007\ Q_{UVB}\ (R^2 = 0.53,\ p < 0.001,\ n = 90) \qquad (4)$$

The combined data represent the largest set of short-term UVBR effects measurements on natural phytoplankton and include phytoplankton sampled from coastal areas, open ocean gyres, equatorial and mid-latitude upwelling areas, the Antarctic convergence, and both surface and deep (20-40 m) samples.

The next largest available data set on marine phytoplankton photoinhibition by UVBR was reported by Smith et al. (1980). They compared dose response regressions based on P.I., CPA, and DNA weighted doses, and found the

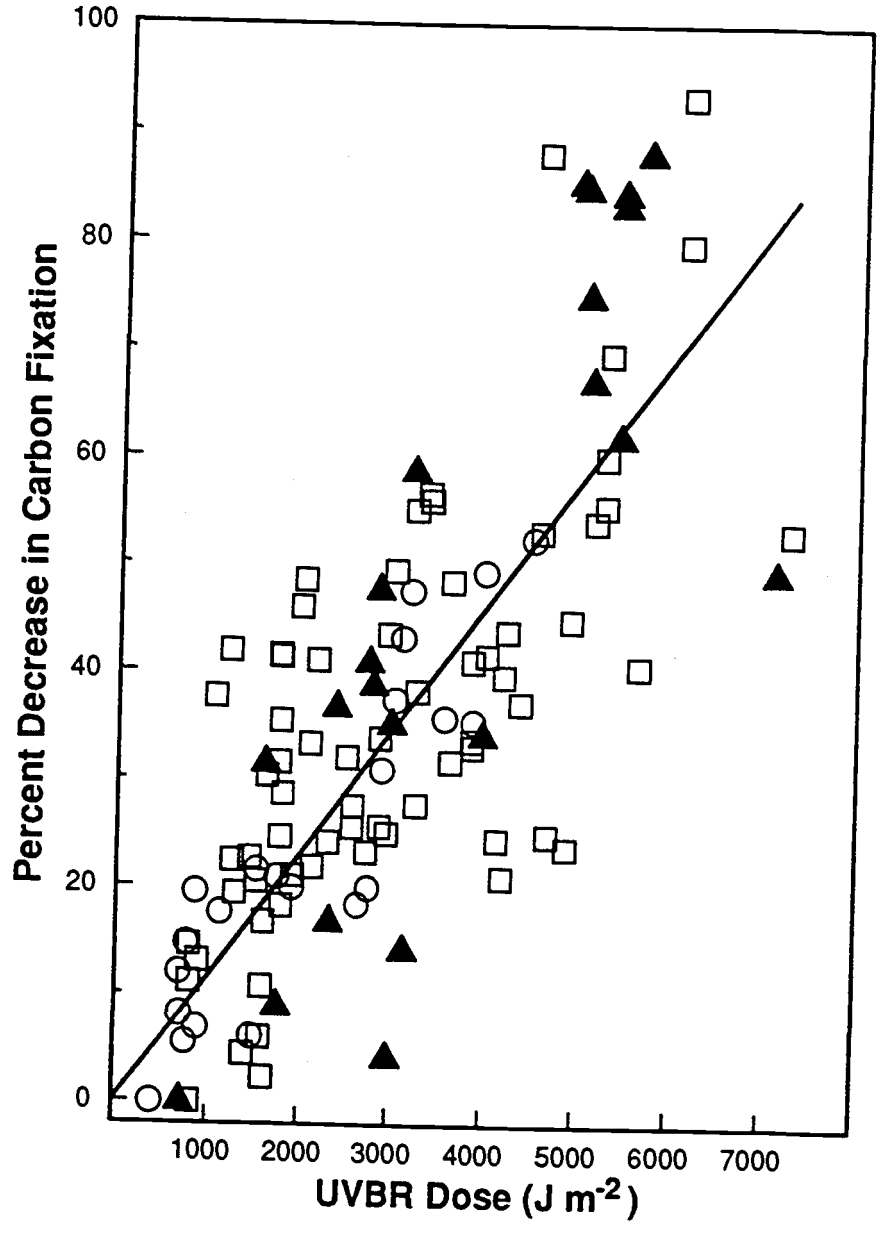

Figure 1-5. Dose response for combined data describing photoinhibition as a function of UVBR doses weighted by the "best fit" action spectrum (n=112, R^2=0.65). O = 1991 data from Washington coast, □ = data from Behrenfeld et al. (1993), and ▲ = ambient treatment data from Smith et al. (1980) converted from P.I. doses to EXP_{300} doses.

greatest convergence between ambient and altered UVBR doses weighted by the P.I. action spectrum. The regression slope for their DNA weighted dose response to solar UVBR (0.018), however, was similar to our slopes using the DNA action spectrum (0.022) and our new action spectrum (0.012, eq. 4). Smith et al. (1980) compared action spectra using data from one experiment (4 data points for each treatment comparison) (Smith et al., Figure 3). We used these data to find a conversion factor to our action spectrum (eq. 2), since the remaining doses were only reported by Smith et al. (1980) as weighted by the P.I. action spectrum.

Conversions of UVBR doses weighted by one action spectrum to another are possible using simple constants when radiation spectra are the same. Conversion of our solar UVBR doses weighted by the P.I. and DNA_{300} action spectrum to doses weighted by our new action spectrum (eq. 2) using the factors 0.095 and 4.296 resulted in standard errors of only ±5% and ±3%, respectively. This error results from variability in the solar spectrum. Lamp UVBR doses weighted by the P.I. action spectrum could be converted exactly to doses weighted by the new action spectrum because lamp spectra are constant.

The conversion factor from the PI action spectrum to the DNA_{300} action spectrum for the four ambient solar data points compared by Smith et al. (1980, Figure 3a and 3c) is 0.010. Current convention is to normalize action spectra

used for UVBR research to 1 at 300 nm. Thus, DNA_{265} UVBR doses reported by Smith et al. (1980) were multiplied by 30.6525 to convert to DNA_{300} doses for calculation of the DNA_{300}:PI conversion factor. Their ambient solar UVBR response data can therefore be converted to doses weighted by the DNA_{300} action spectrum by multiplying each dose by 0.010. Our data provides the factor 4.296 to convert DNA_{300} doses to doses weighted by our new action spectrum. The dose response to solar UVBR based on the P.I. action spectrum as reported by Smith et al. (1980) therefore can be converted to a dose response based on our new action spectrum by multiplying each P.I. dose by 0.010 to convert to DNA_{300} doses and 4.296 to convert DNA_{300} doses to doses weighted by the action spectrum described by (eq. 2). The converted ambient UVBR dose response data of Smith et al. (1980) thus closely correspond to our dose response data (Fig. 1-5) and result in a higher regression coefficient (R^2 = 0.65) for the combined data.

The dose response slope for the 4 enhanced UV observations used by Smith et al. (1980, Figure 3a) for their action spectrum comparison does not correspond to the slope of our dose response. This discrepancy may have been due to spectral differences between their lamp enhancements and ours. Smith et al. (1980) used FS40 Westinghouse ultraviolet fluorescent lamps to enhance the UVBR dose above ambient. Lamp UV enhancement can be estimated as the

difference between the total enhanced dose and the ambient dose weighted by the P.I. and DNA action spectra (Smith et al., 1980, Figure 3a and 3c). Our estimated ratio of their lamp DNA:P.I. weighted UVBR doses is 1.94, after converting from DNA_{265} to DNA_{300} doses. DNA_{300}:P.I. dose ratios for unfiltered FS40 Westinghouse lamps and filtered by cellulose triacetate measured in our laboratory were 1.86 and 0.51, respectively. Unfiltered UV lamp radiation represents a much greater biologically effective dose than filtered lamp radiation under the DNA_{300} action spectrum but not the P.I. action spectrum, thus a higher DNA:P.I. dose ratio. Therefore, we believe that the 4 responses to enhanced UVBR used by Smith et al. (1980) for comparison of action spectra were for unfiltered FS40 lamps and included lamp radiation <290 nm (as indicated by the high DNA_{300}:P.I. ratio). Complete re-evaluation could not be made for the remaining altered treatment data of Smith et al. (1980) because UVBR excluded results could not be distinguished from the UVBR enhanced results.

Our results and the dose responses reported previously (Smith et al., 1980; Behrenfeld et al., 1993) are similar when comparisons are limited to the UVBR waveband. Divergence occurs when wavelengths <290 nm are included in the enhanced treatments, indicating that neither our new action spectrum or the DNA action spectrum adequately

describe the effectiveness of wavelengths <290 at causing photoinhibition of carbon fixation in marine phytoplankton.

Threshold for UVBR Effects

We assumed that linear responses to UVBR occur within any given wavelength and, therefore, to any constant spectrum. Lamp spectra remain constant during the course of any experiment. Lamp spectra are also the same between experimental studies. In contrast, the solar spectrum changes constantly with time, place, and atmospheric conditions. The small deviations from linearity in dose responses that occurred under lamp spectra (Fig. 1-1a: ▲) compared to the deviations from linearity that occurred under solar spectra (Fig. 1-1a: □) appear to support our assumption. Thus, without an *a priori* reason for assuming more complex dose responses to UVBR, a linear response to UVBR by marine phytoplankton appears to be the most parsimonious assumption.

Rejection of a linear dose response to UVBR (e.g., Helbling et al., 1992) is unwarranted without testing spectral data for a wavelength specific response (i.e., use of an action spectrum). A sigmoid dose response could be fit to the unweighted solar data presented here (Fig. 1-1a), suggesting a threshold effect. Evidence for such a sigmoidal response is highly dependent upon the response at

the lowest UVBR intensity, which occurred on the most heavily overcast day. On overcast days, short UVBR wavelengths are attenuated more than longer wavelengths. The biologically effective dose is then lower per unit UVBR energy than during a clear day. This discrepancy is accounted for by using the "best fit" action spectrum.

CONCLUSIONS

Short-term photoinhibition of carbon fixation by UVBR appears to be a linear function of total dose. The wavelength specific biological effectiveness of UVBR in reducing carbon fixation is adequately described by a simple exponential action spectrum (eq. 2). However, the exponential action spectrum applies only to the UVBR waveband. The biological effectiveness of wavelengths shorter than 290 nm will not continue to increase exponentially (Quaite et al., 1992) and damaging efficiency may not continue to decrease exponentially for wavelengths greater than 320 nm. Ultraviolet-A radiation (321-400 nm) induced photoinhibition in the ocean surface has been noted (Bühlmann et al., 1987; Helbling et al., 1992; Smith et al., 1991). Recently, two additional action spectra for photoinhibition of phytoplankton photosynthesis by UVBR have been reported (Cullen et al., 1992; Lubin et al., 1992). The spectrum of Lubin et al. (1992) is not dissimilar to the DNA or exponential action spectra for the UVBR waveband and lends support to our conclusions. Finally, the lack of a threshold in our dose response (Fig. 1-3) does not imply that adaptive mechanisms are not important. Indeed, much of the scatter around the regression (Fig. 1-5) could be due to differences in the UVBR tolerances of the phytoplankton sampled during any one experiment.

Depletion of the stratospheric ozone layer results in a proportionately larger increase in short UVBR wavelengths than in longer wavelengths (Green et al., 1980). The steep slope of our new action spectrum indicates that this increase in UVBR would represent a significant increase in the biologically damaging dose at sea level. Alternatively, if UVBR photoinhibition of marine phytoplankton fits a P.I. type action spectrum, then stratospheric ozone depletion would result in only a small increase in biologically effective dose at the sea surface. However, short wavelengths of UVBR are attenuated more rapidly in the oceans' surface than longer wavelengths (Zaneveld, 1975) and, therefore, attenuation of biologically effective dose would be much more rapid for doses weighted by our exponential action spectrum than a P.I. type action spectrum.

CHAPTER 2: INHIBITORY EFFECTS OF ULTRAVIOLET-B RADIATION ON NO_3^- AND NH_4^+ UPTAKE BY NATURAL PLANKTON ASSEMBLAGES FROM THE NORTH PACIFIC OCEAN: ACTION SPECTRUM AND DOSE RESPONSE

by: Michael J. Behrenfeld, David R.S. Lean, and Henry Lee II

ABSTRACT

Ammonium uptake (ρ_{NH4}) by natural plankton assemblages from the North Pacific was inhibited by ultraviolet radiation (UVR) to a greater extent than nitrate uptake. The action spectrum for ρ_{NH4} inhibition had a lower slope and greater relative contribution from wavelengths >320 nm to total biologically effective dose than the action spectrum for UVR inhibition of carbon fixation. Inhibition of ρ_{NH4} was a linear function of UVR dose weighted by the new action spectrum. Comparison between dose-responses and action spectra for ρ_{NH4} and carbon fixation indicate deeper penetration of UVR effects on ammonium uptake than carbon uptake.

ACKNOWLEDGEMENTS

The authors thank the crew of the R.V. Discoverer, Dave Wisegarver and Dr. John Bullister without whose help this research would not have been possible. We also thank J. Chapman, M.L. Dixon, G. Garber, and L.F. Small for helpful suggestions on the manuscript.

This research was funded by the USEPA under contract 68-CO-0051 and represents EPA:ERL-N contribution number 1458.

INTRODUCTION

Primary production in the ocean surface can be inhibited by high intensities of solar radiation (Kyle et al., 1987). The contribution of ultraviolet-B radiation (UVBR: 290-320 nm) to total surface photoinhibition has become an increasing concern due to enhanced UVBR resulting from stratospheric ozone depletion (Smith et al., 1980; Bidigare, 1989; Voytek, 1990; Helbling et al., 1992; Smith et al., 1992; Behrenfeld et al., 1993). Integrated UVBR energy constitutes only a small fraction of the total energy of solar ultraviolet radiation (UVR: <400 nm). However, effectiveness of UVR in causing biological damage increases with decreasing wavelength (Jones and Kok, 1966; Caldwell, 1971; Setlow, 1974; Quaite et al., 1992; Cullen et al., 1992; Behrenfeld et al., 1993). UVBR thus contributes a large fraction of total biologically effective solar dose when the wavelength-specific response is steeply weighted toward the shortest UVR wavelengths.

Action spectra are arithmetic descriptions of the wavelength dependency for biological effect. Action spectrum slope is dependent upon the biological process being measured (e.g., carbon fixation, growth inhibition, etc.). Knowledge of the appropriate action spectrum for UVBR inhibition of a given biological process allows comparison of dose responses to UVBR exposures of variable

spectral quality. However, difficulties in determining action spectra have prevented the development of action spectra specific for each biological process. Thus, early studies of UVBR effects on marine phytoplankton utilized action spectra derived from bacteria and phages (Setlow, 1974), terrestrial plants (Caldwell, 1971), or cellular extracts (Jones and Kok, 1966). Recently, a phytoplankton-specific action spectrum was determined from carbon uptake rates in monocultures of the diatom *Thalassiosira pseudonana* (Cullen et al., 1992). All of these action spectra were determined during laboratory studies using physiological responses to small incremental changes in electromagnetic radiation spectra (the "incremental" method). The "incremental" method results in action spectra with high wavelength resolution, but these action spectra are difficult to extrapolate to natural phytoplankton communities with whole cells and mixed species.

Results described in chapter 1 present an alternative to the "incremental" method which allows determination of action spectra from field-collected dose-response data. The action spectrum for UVR inhibition of carbon uptake (Chapter 1) was determined by changing the slope of an exponential curve until responses to spectrally distinct UVR doses converged into a single, linear dose-response. The action spectrum was derived from natural populations, thus avoiding uncertainties associated with extrapolation from laboratory

results. The action spectrum for carbon fixation (Chapter 1) lacks the spectral resolution of the "incremental" method and becomes less precise as differences between treatments occur over an increasing range of wavelengths.

Inhibitory effects of a spectral or intensity shift in UVBR on phytoplankton productivity can be modeled using the dose-response and action spectrum for carbon fixation (Chapter 1). However, a different estimate of inhibition may result if the action spectrum and dose-response used for the model were based upon a biological process other than carbon uptake. We measured the inhibitory effects of solar and artificially enhanced UVR on NO_3^- and NH_4^+ uptake by natural plankton assemblages from the North Pacific Ocean. An action spectrum and dose-response was determined for UVR inhibition of NH_4^+ uptake using methods outlined by Behrenfeld et al. (1993a). Our results are compared to earlier studies on action spectra and dose-responses for UVR inhibition of nitrogen and carbon uptake.

MATERIALS AND METHODS

Nitrogen Uptake Measurements

Twelve UVR exposure experiments were conducted during March and April, 1991 between 37°N and 55°N on board the NOAA R.V. Discoverer (Fig. 2-1). Samples for nutrient and particulate organic nitrogen (PON) analysis were collected for each nitrogen uptake experiment. NO_3^-, NO_2^-, $Si(OH)_4$, and PO_4^{-3} concentrations were determined using standard autoanalyzer techniques. NH_4^+ was measured using the phenolhypochlorite method (Strickland and Parsons, 1972). PON concentration was determined by filtering 1.5 - 2.5 L of seawater onto 25 mm Whatman GF/F filters (pre-combusted at 450°C for 15 min), freezing the filters over desiccant, and analyzing for PON at a shore-based laboratory using a Perkin-Elmer 240C Elemental Analyzer calibrated with acetanilide and chlorodinitrobenzene.

Phytoplankton samples for nitrogen uptake experiments were collected before sunrise from <2 m depth using a clean bucket. Samples were immediately dispensed into 500 ml UVBR-transparent FEP Teflon^R bottles and inoculated with $^{15}NH_4^+$ (99.7 atom% [$^{15}NH_4^+$] as ammonium chloride) or $^{15}NO_3^-$ (98.8 atom% [$^{15}NO_3^-$] as sodium nitrate). $^{15}NO_3^-$ was added at approximately 10% ambient NO_3^- concentrations. $^{15}NH_4^+$ was added at a "trace" concentration of 0.1 μM. After ^{15}N

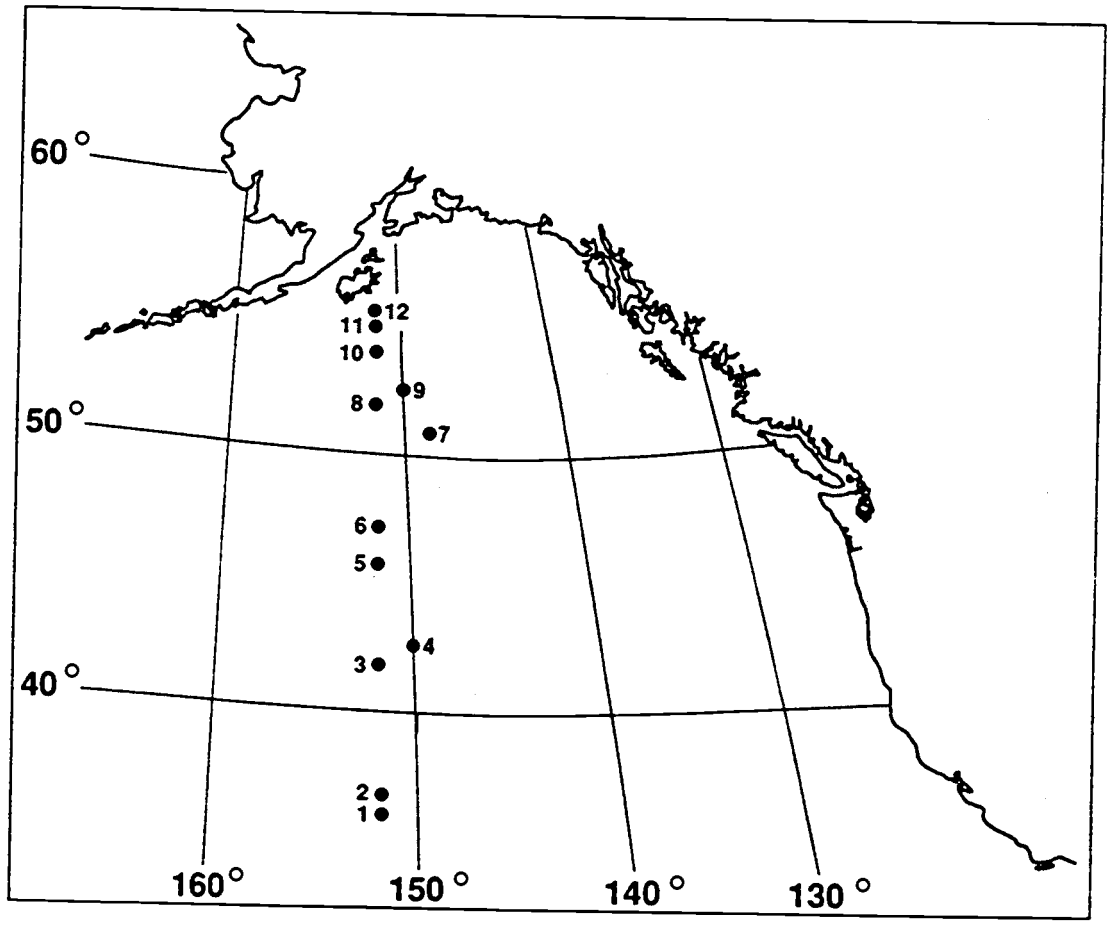

Figure 2-1. Sampling stations during the 1991 cruise in the North Pacific.

inoculation, samples were incubated for 4.6 - 8.5 hrs in an on-deck incubator (Behrenfeld et al., 1993). Ten replicate samples were used in each of 3 treatments: 1) UVBR <315 nm excluded, 2) ambient UVR, and 3) UVR >290 nm enhanced above ambient. Flow-through seawater maintained samples at sea surface temperature.

Following incubation, samples were filtered at 70 kPa through a 25 mm Whatman^{R} GF/F filter (pre-combusted at 500°C for 15 min.) at 1 L per filter (i.e., two 500 ml bottles per filter). Thus, 5 replicate filters were collected for each UVBR treatment. Filters were immediately frozen and later dried at 60°C for 2 hrs prior to ^{15}N analysis. Dried filters containing ^{15}N-labeled particulate material were placed into discharge tubes with CuO powder as a catalyst. Tubes were sealed after evacuation to 0.01 Pa, combusted at 590°C for 16 hr, and allowed to cool for 24 hr. Atom percent excess ^{15}N of the particulate material was measured using a Jasco emission spectrometer (NAJI-1) (Murphy, 1980). Absolute uptake rates (ρ) of NO_3^- and NH_4^+ were calculated as:

$$\rho = \frac{\text{atom\% excess } ^{15}N \text{ of filtered sample} * \text{PON}}{\text{atom\% enrichment of } ^{15}NH_4^+ \text{ or } ^{15}NO_3^- * \text{incubation time}}$$

Specifics of Ultraviolet Treatments

Ultraviolet fluorescent lamps (UVB 313, Q-Panel Co.), pre-burned for approximately 100 hrs, were used to create the UVR-enhanced treatment. Lamps were located beneath a UVR-transparent acrylic incubation tank (Acrylite OP-4, CYRO Industries). Cellulose acetate (0.13 mm) between the lamps and the UVR-enhanced treatment bottles eliminated lamp radiation <290 nm. Mylar^{R} (0.13 mm) placed between the lamps and all other bottles eliminated lamp radiation <315 nm. Neutral density screen was used to adjust the intensity of UVR enhancement. Bottles in the UVBR-excluded treatment were wrapped with Mylar^{R} to eliminate solar wavelengths <315 nm. Cellulose acetate and Mylar^{R} films were replaced periodically to avoid photodegradative changes in transmittance properties. Measured spectra in the UVBR-excluded, ambient-UVR, and UVR-enhanced treatments are shown in figure 2-2.

Ambient solar radiation (285-800 nm) was continuously monitored using an Optronic Model 752 spectroradiometer. The spectroradiometer was calibrated for wavelength offset by scanning a mercury arc lamp, and for intensity using a halogen lamp traceable to the National Institute of Standards and Technology. The calibrated spectroradiometer has a reported wavelength accuracy of ±0.3 nm, wavelength precision of ±0.1 nm, and an intensity accuracy of ±2-4%.

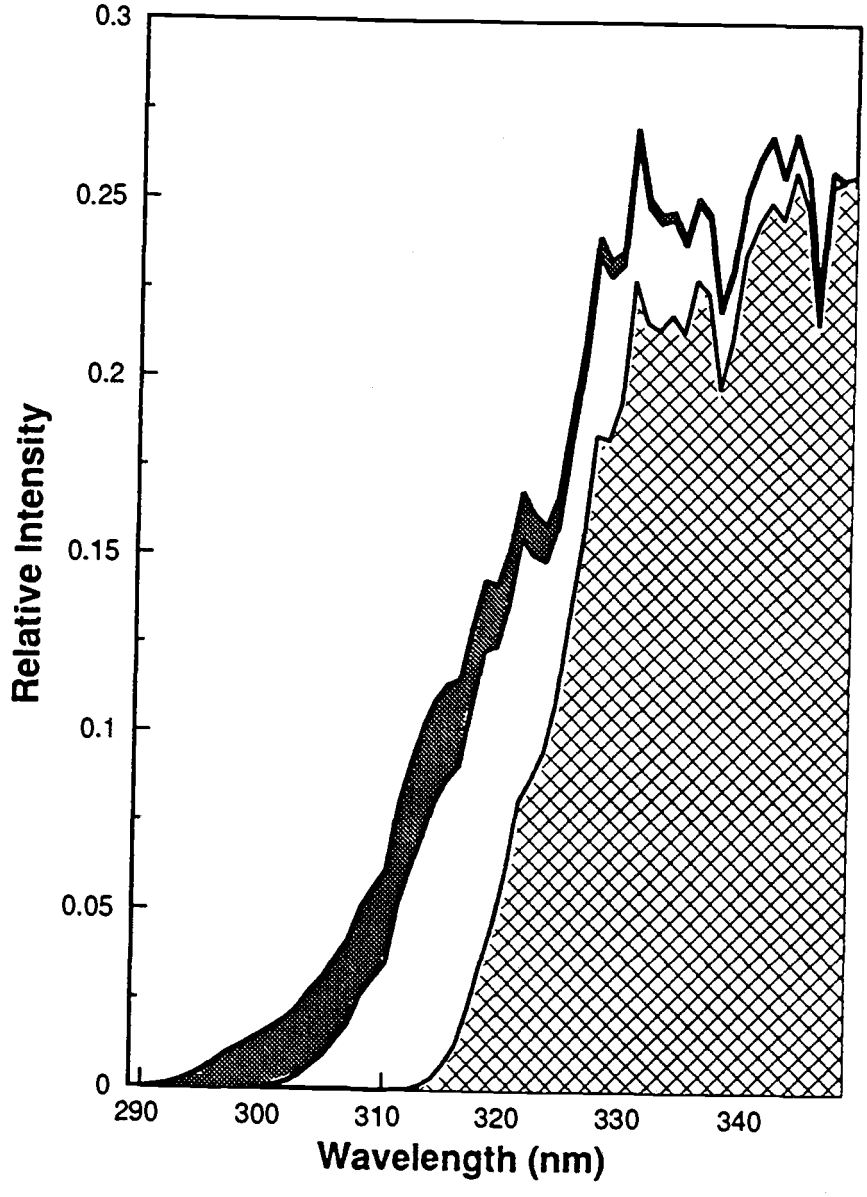

Figure 2-2. Measured spectra in the UVBR-excluded (cross hatch), ambient-UVR (unshaded) and UVR-enhanced (dark shade) treatments.

The spectroradiometer was also used to measure lamp UVR doses in the incubation tanks.

RESULTS

Samples for the UVR-exposure experiments were collected from three hydrographically distinct regions. Stations 1 and 2 corresponded to the northern boundary of the North Pacific gyre (<42°N), as indicated by a shallower thermocline, warmer surface water (Fig. 2-3), and low ambient nutrient concentration (Fig. 2-4). A transition zone existed between 42°N and 50°N (stations 3-6), exhibiting decreasing surface water temperatures, deepening of the surface mixed layer (Fig. 2-3), and increasing $Si(OH)_4$, NO_3^-, and PO_4^{-3} concentrations. Samples collected from >50°N (stations 7-12) corresponded to the high-nutrient (Fig. 2-4), deeper-mixing (Fig. 2-3) Subarctic North Pacific. The surface salinity minimum characteristic of the North Pacific was evident at latitudes >39°N (not illustrated).

Nitrate uptake rates (ρ_{NO3}) were lowest (<0.16 nM l^{-1} hr^{-1}) in the North Pacific Gyre then increased gradually to >1.0 nM l^{-1} hr^{-1} in the Subarctic North Pacific (Fig. 2-5a). Ammonium uptake rate (ρ_{NH4}) in the UVBR-excluded treatment was highest ($0.49<\rho_{NH4}<0.64$ nM l^{-1} hr^{-1}) in the transition zone and at the station nearest to Kodiak Island, Alaska (station 12; ρ_{NH4} = 0.80 nM l^{-1} hr^{-1}) (Fig. 2-5b).

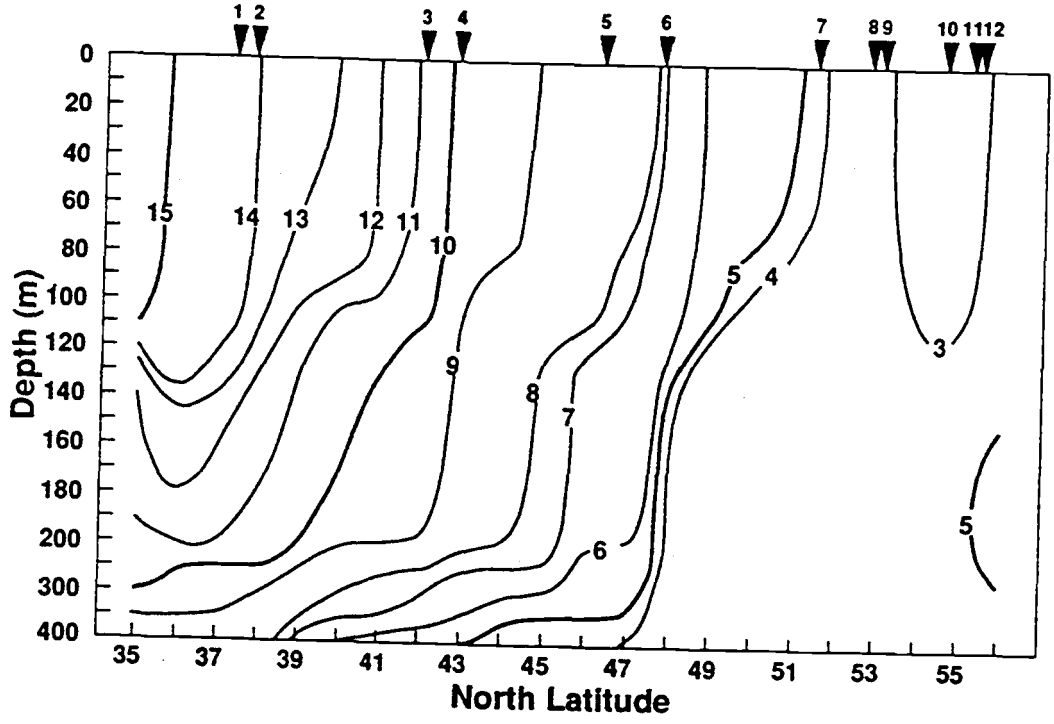

Figure 2-3. Vertical profile of potential temperature (°C) following 152°W longitude. Sampling stations identified in Fig. 1 are indicated at the top. (Data provided by PMEL, NOAA).

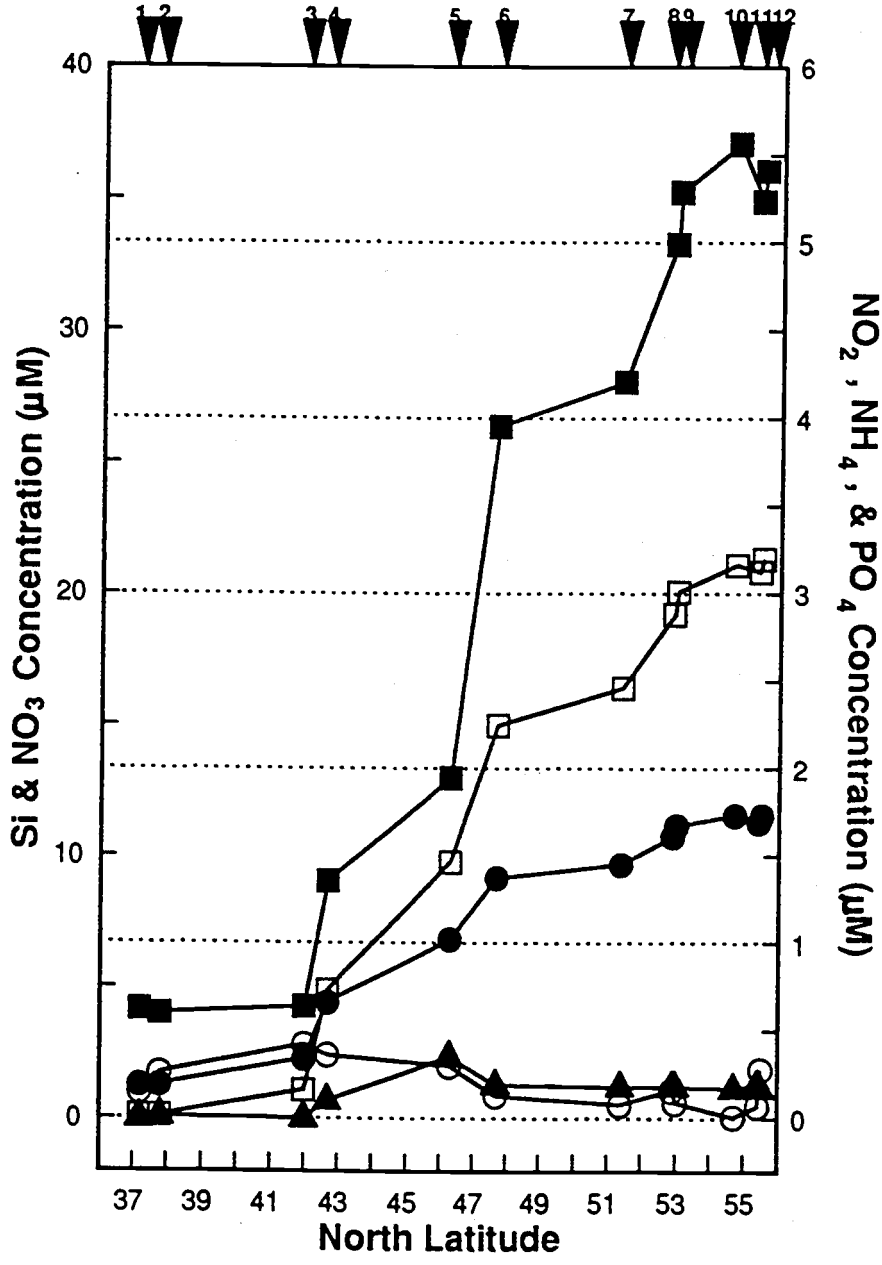

Figure 2-4. Ambient nutrient concentrations (µM) at each sampling station indicated in Fig. 1. □ = NO_3^-, ▲ = NO_2^-, O= NH_4^+, ■ = Si, ● = PO_4^{-3}. (Data provided by PMEL, NOAA).

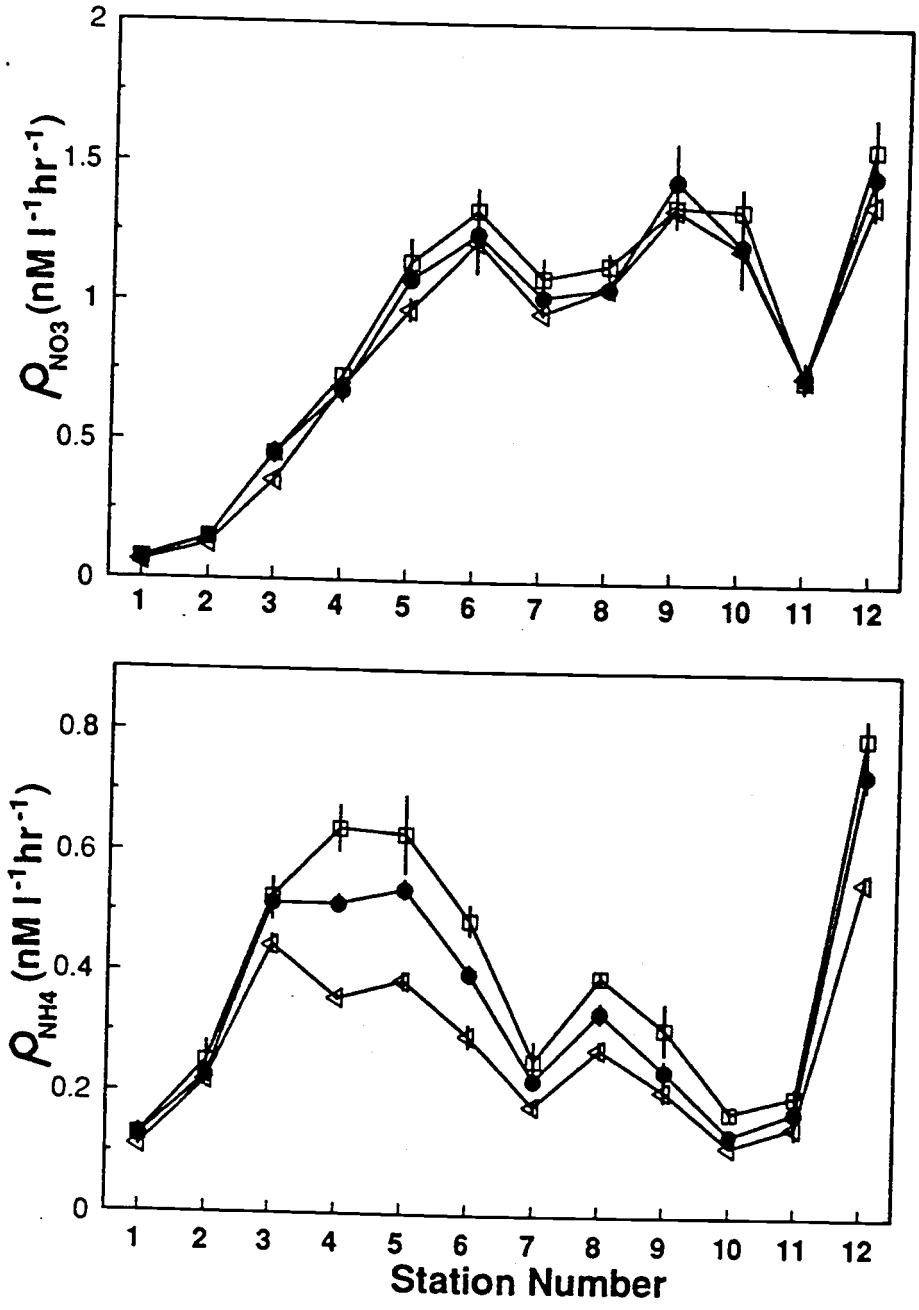

Figure 2-5. Absolute uptake rates of (A) nitrate (ρ_{NO3}) and (B) ammonium (ρ_{NH4}) (nM l^{-1} hr^{-1}) in the UVBR-excluded (□), ambient-UVR (●), and UVR-enhanced (▲) treatments at each sampling station.

UVR inhibition of nitrogen uptake

Nitrate uptake (ρ_{NO3}) was reduced on average 4% in the ambient-UVR treatment and 10% in the UVR-enhanced treatment compared to ρ_{NO3} in the UVBR-excluded treatment (Fig. 2-5a). However, treatment differences for any given experiment were often insignificant ($p>0.05$) despite very low within-treatment variability (Fig. 2-5a). Treatment differences remain insignificant with or without weighting the UVR by an action spectrum. Thus, no significant effect of UVR on ρ_{NO3} could be detected within the sensitivity of the methods used during these experiments.

In contrast, treatment differences in ρ_{NH4} were significant ($p < 0.05$) at nearly every station (Fig. 2-5b). Decreases in ρ_{NH4} of 2% to 22%, relative to the UVBR excluded treatment, resulted from unweighted solar UVR doses of 12.6 to 37.5 kJ m^{-2}. Unweighted UVR doses in the enhanced treatment (18.4 to 47.6 kJ m^{-2}) decreased ρ_{NH4} by 24% to 44% compared to the excluded treatment. Percent decrease in ρ_{NH4} per unit unweighted UVR dose was greater in the enhanced-treatment than in the ambient-treatment. Enhanced-treatment spectra were enriched in short UVBR wavelengths relative to the solar spectrum (Fig. 2-2). Thus, greater decreases in ρ_{NH4} per unit UVR dose in the enhanced-treatment were due to short wavelengths having greater damaging efficiency than longer wavelengths.

UVR doses must be weighted by an action spectrum when calculating a dose-response from combined data of spectrally distinct treatments if the measured response is wavelength dependent. An action spectrum for UVR inhibition of ρ_{NH4} can be calculated from the ambient and enhanced dose-response data using the exponential model of Behrenfeld et al. (1993a):

$$\text{Action spectra} = \alpha e^{c\lambda} \qquad (1)$$

where; c is the action spectrum slope, λ is wavelength, and α is a normalization factor. The action spectrum for ρ_{NH4} inhibition is determined from equation (1) by varying "c" until the independently calculated dose-response slopes and intercepts of each treatment converge. The action spectrum for ρ_{NH4} inhibition, normalized to 1 at 300 nm (i.e., EXP_{N300}) was:

$$EXP_{N300} = 1.161*10^{8}\ e^{-0.0619\lambda} \text{ (Fig. 2-6)} \qquad (2)$$

Equation (2) describes the mean wavelength dependency of ρ_{NH4} inhibition between 290 and 346 nm (i.e., the wavelength range of spectral divergence between treatments), but does not account for variability on a per-nanometer scale. Action spectra calculated from equation (1) assume the measured response is a linear function of dose for any given wavelength and, therefore, any constant spectrum.

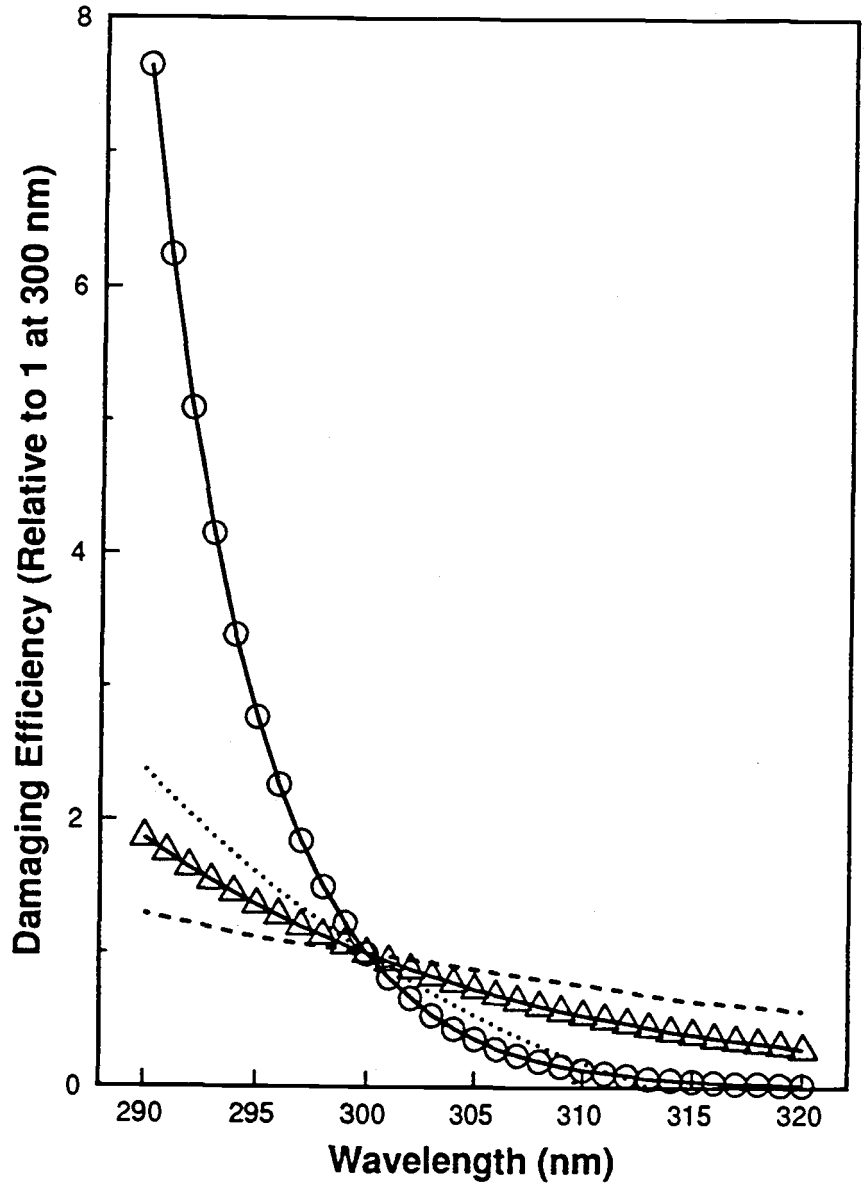

Figure 2-6. Action spectra for UVBR inhibition of ρ_{NH4} (-Δ-Δ-) (eq. 2), carbon fixation (-O-O-) (Chapter 1), and the Caldwell Plant Action spectrum (·····) (Caldwell, 1971). The Photoinhibition action spectrum (-----) (Jones and Kok, 1966) was used by Smith et al. (1980) to describe UVR inhibition of phytoplankton carbon fixation and is included for comparison. Damaging efficiency of all action spectra relative to 1 at 300 nm.

Decreases in ρ_{NH4} relative to the UVBR-excluded treatment measured during the first three experiments were divergent from the remaining data (Fig. 2-7) and were not used in the calculation of an action spectrum. Differences between ρ_{NH4} in the ambient-UVR and UVR-enhanced treatments at stations 1-3, however, had a similar dose-response slope to those measured at all other stations (Fig. 2-7), and were included in the calculation of an action spectrum. Similarity of dose-responses between the ambient-UVR and UVR-enhanced treatments at stations 1-3 and those measured at all other stations suggests that divergence of responses relative to the UVBR-excluded treatment at stations 1-3 were due to underestimation of ρ_{NH4} in the UVBR-excluded treatment, but may have been due to tolerance of phytoplankton at these three stations to ambient UVBR.

Excluding ρ_{NH4} data from the UVBR-excluded treatment of the first three experiments, the dose-response for UVR inhibition of ρ_{NH4} was:

$$PI_{NH4} = 0.00288\ Q_{EXP}\ (R^2 = 0.77,\ p<0.001,\ n=21)\ \text{(Fig.2-7)} \quad (3)$$

where; PI_{NH4} is percent inhibition of ρ_{NH4} relative to the UVBR-excluded treatment (station 4-12) or ambient-UVR treatment (station 1-3) and Q_{EXP} is UVR dose (J m^{-2} EXP_{N300}) weighted by the action spectrum for ρ_{NH4} inhibition described in equation (2).

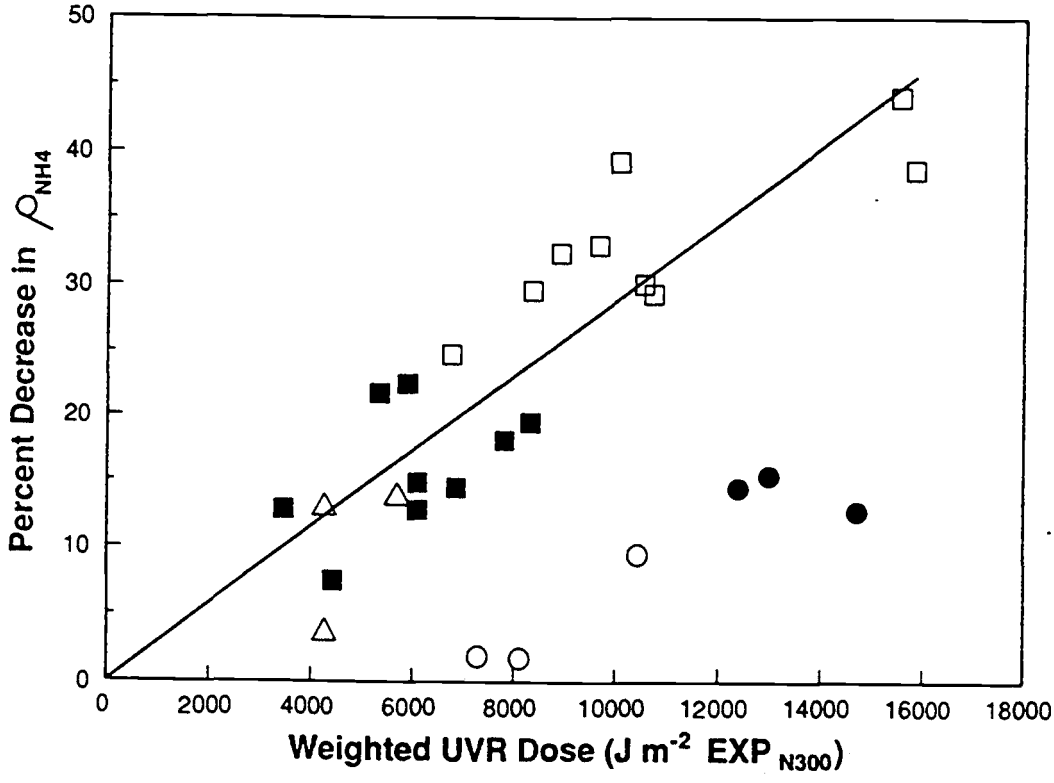

Figure 2-7. Percent decrease in ρ_{NH4} as a function of total UVR dose weighted by the exponential action spectrum (eq. 2). Divergent responses, relative to the UVBR-excluded treatment, of the first three stations are indicated by o for the ambient-UVR and ● for the UVR-enhanced treatments. Percent decrease between ambient-UVR and UVR-enhanced treatments for first three stations indicated by ▵. Response for all other stations indicated by ■ for ambient-UVR and □ for UVR-enhanced treatments.

DISCUSSION

Exposure of natural plankton assemblages to different UVR intensities and spectra decreased ρ_{NO3} less than ρ_{NH4}. Greater sensitivity of ρ_{NH4} to UVR exposure was also reported by Döhler (1987, 1988) for monocultures and natural assemblages of marine phytoplankton. We found inhibition of ρ_{NH4} by UVR in natural plankton assemblages to be a linear function of cumulative biologically effective dose (eq. 3), explaining 77% of the variability between UVR treatments.

Effectiveness of UVR at inhibiting ρ_{NH4} decreases with increasing wavelength between 290 and 346 nm (eq. 2). Slope of the action spectrum for ρ_{NH4} inhibition (eq. 2) is roughly a factor of three lower than the slope for UVR inhibition of carbon fixation (Chapter 1) (Fig. 2-6). Thus, photoinhibition of carbon fixation is dominated by wavelengths <320 nm, while UVAR contributes significantly to photoinhibition of ρ_{NH4}. Slope of the action spectrum for ρ_{NH4} is intermediate to the Caldwell Plant Action spectrum (CPA) (Caldwell, 1971) and the Photoinhibition action spectrum of Jones and Kok (1966) (Fig. 2-6). Döhler (1987, 1988) described UVR inhibition of nitrogen uptake using the CPA spectrum. The CPA spectrum, which was determined for inhibition of photosynthesis in terrestrial plants, assigns a biological weight only to wavelengths ≤313 nm and has a steeper slope than our action spectrum for inhibition of

ρ_{NH4}. Thus, our results and those of Döhler (1987, 1988) differ with respect to the wavelength specificity of ρ_{NH4} inhibition.

Importance of UVAR in ρ_{NH4} inhibition implies that careful characterization of spectral differences in UVAR between treatments should be made during UVBR effects studies on ρ_{NH4}. Imperfect cutoff characteristics of spectral filters such as Mylar^R can result in significant differences in biologically effective UVAR doses between treatments (Fig. 2-2). Similar differences in UVAR intensity between treatments would be less important for metabolic processes such as carbon fixation which have steeply sloped action spectra in the UVBR waveband and only a small contribution to biologically effective dose from UVAR wavelengths.

Differences between action spectra for ρ_{NH4} (eq. 2) and carbon fixation (Chapter 1) have important implications on depth integrated estimates of UVR effects. Attenuation rate of UVR increases with decreasing wavelength (Zaneveld, 1975; Smith and Baker, 1981). Biologically effective dose based on the steeply sloped action spectrum for carbon fixation is attenuated more rapidly than for metabolic processes such as ρ_{NH4} which are inhibited to a relatively greater extent by deeper penetrating UVAR wavelengths. Attenuation of UVR in the water column is roughly the sum of four attenuating components; water, salts, dissolved organic matter (DOM),

and particulates (including phytoplankton) (Kirk, 1983). UVR attenuation by water is fairly constant for the range of salinities found in most oceanic regions. The contribution of DOM to UVR attenuation is greatest in coastal regions where DOM concentrations are high. Thus, the maximum effects of UVR based on the action spectra and dose-responses for either carbon fixation or ρ_{NH4} should occur in offshore regions with high surface phytoplankton concentrations and low DOM. Such conditions would maximize the fraction of subsurface UVR absorbed by phytoplankton and minimize absorption by water and DOM. In contrast, UVBR absorption in optically clear oceanic regions is due primarily to water rather than particulates.

Our action spectrum and dose-response for inhibition of ρ_{NH4} are based on short-term (4.6-8.5 hrs) uptake measurements and may not be representative of longer-term effects on growth and biomass. Short-term measurements of UVR inhibition may also underestimate the importance of nutritional status of the cells (Cullen and Lesser, 1991; Chapter 3). Small-volume deck incubations likely involve significant experimental artifacts and may not be representative of true open ocean processes. Exposure to extremely high intensities of solar radiation (a common problem with deck incubations) may not have been an important factor in the current study since skies were overcast during 8 of the 12 experiments and partially cloudy

during 3 of the remaining 4 experiments. Finally, some of the variability in ρ_{NH4} between UVR treatments not explained by the cumulative UVR dose (eq. 3) may have been due to differences in UVR dose-rates (Cullen and Lesser, 1991; Cullen et al., 1992).

Photosynthetic carbon fixation, as measured by radiolabeled carbon uptake, has been the primary method for estimating the effect of UVBR on surface phytoplankton productivity (e.g., Lorenzen, 1979; Smith et al., 1980; Maske, 1984; Bühlmann et al., 1987; El Sayed et al., 1990; Smith et al., 1992; Behrenfeld et al. 1993, Chapter 1). Effects of UVR on nitrogen uptake suggest deeper penetration of UVR photoinhibition. Equating decreased surface ρ_{NH4} to changes in carbon uptake rate is problematic because ammonium is not the only form of nitrogen available to phytoplankton and UVR effects on the uptake rate of at least one of these forms (nitrate) is dissimilar to the effect on ρ_{NH4}. Decreases in ρ_{NH4} and carbon uptake rates may be comparable in oceanic regions where NH_4^+ is the overwhelmingly predominant nitrogen source. Insensitivity of ρ_{NO3} to UVR may compensate for effects on ρ_{NH4} when surface NO_3^- is available. Expanding the number of metabolic processes used in UVBR studies will enhance our understanding of the photoinhibitory role of UVBR in the oceans surface and improve our ability to predict the effects of increasing UVBR on phytoplankton productivity.

CHAPTER 3: A COMPETITIVE INTERACTION BETWEEN NUTRITIONAL STATUS AND ULTRAVIOLET-B RADIATION EFFECTS ON A MARINE DIATOM

by: Michael J. Behrenfeld, Henry Lee II, and Lawrence F. Small

ABSTRACT

Influence of nutritional status on the photoinhibitory effects of ultraviolet-B radiation (UVBR: 290-320 nm) on specific growth rates (μ_{obs}) and biomass of *Phaeodactylum tricornutum* were determined using nutrient-replete batch cultures and nutrient-limited continuous cultures. *P. tricornutum* cultures were exposed to UVBR doses representative of mid-latitude and ozone depletion intensities. Specific growth rates and biomass were inhibited from 2% to 16% by UVBR during nutrient-replete growth. However, no effect of UVBR was detectable when inhibition of μ_{obs} and biomass by nutrient limitation exceeded the potential for inhibition by UVBR. Thus, a competitive interaction appears to occur between macronutrient stress and UVBR stress, such that μ_{obs} and biomass will be determined by the most limiting factor (i.e., Liebig's "law" of the minimum). Results suggest that phytoplankton in nutrient-rich areas of the ocean may be most susceptible to UVBR inhibition of growth and biomass, while these parameters may not be appropriate for measuring UVBR stress in regions of nutrient limitation.

ACKNOWLEDGEMENTS

We thank John Chapman, Karl Rukavina, David Specht, Anne Sigleo, John Hardy, Henry Walker, Dave Nelson, and John Cullen for aid in experimental design and execution and for constructive reviews of the manuscript aid in experimental design and execution. We also thank Louis Gordon, Andrew Ross, and Sandy Moore for analysis of nutrients and particulate carbon and nitrogen.

This research was funded by the USEPA under contract 68-CO-0051 and represents EPA:ERL-N contribution number N238.

INTRODUCTION

Phytoplankton in the upper euphotic zone of oceans and lakes exhibit variable degrees of photoinhibition during periods of peak irradiance (Kyle et al., 1987). Photoinhibition can be induced by short wavelengths of ultraviolet radiation (UVR) (Lorenzen, 1979; Smith et al., 1992) or high intensities of photosynthetically active radiation (PAR) (Neale, 1987). The fraction of total surface photoinhibition that can be attributed to the narrow waveband of ultraviolet-B radiation (UVBR: 290-320 nm) has recently been the topic of much research due to increases in surface UVBR resulting from stratospheric ozone depletion (Lubin et al., 1989; Stolarski et al., 1992).

Measured decreases in short-term (<12 hr) photosynthetic carbon uptake provide evidence that natural phytoplankton assemblages are inhibited by ambient solar UVBR and enhanced UVBR (Smith et al., 1980; Helbling et al., 1992; Behrenfeld et al. 1993, Chapter 1). Photoinhibition of carbon fixation by UVBR has been documented in oceanic regions ranging from oligotrophic to highly productive (Behrenfeld et al. 1993, Chapter 1). Smith et al. (1992) used short-term dose responses of Antarctic phytoplankton to UVBR to estimate effects of ozone depletion on primary production. However, it is unclear whether dose-response models based on short-term carbon uptake measurements (Smith

et al., 1980; Smith et al., 1992; Behrenfeld et al., 1993; Chapter 1) are indicative of the long-term photoinhibitory potential of UVBR on phytoplankton growth and biomass. Interactions between UVBR stress and other environmental stresses which limit phytoplankton growth (e.g., micro- or macro-nutrients) are perhaps the greatest uncertainties for modeling UVBR effects on phytoplankton productivity.

Measurements of UVBR inhibition of phytoplankton growth and biomass have been limited almost entirely to laboratory studies using phytoplankton monocultures (Calkins and Thordardottir, 1980; Thomson et al., 1980; Wolniakowski, 1980; Worrest et al., 1981a; Döhler, 1984a; Döhler, 1984b; Jokiel and York, 1984; Döhler et al., 1987; Ekelund, 1990; El-Sayed et al., 1990; Helbling et al., 1992; Behrenfeld et al., 1992). Exposure of phytoplankton to UVBR typically results in decreased specific growth rates (μ_{obs}) and biomass. The extent of UVBR inhibition is dependent upon temperature (Döhler, 1984a), light history (Zifka et al., 1992), and the phytoplankton species used during the study. Laboratory studies often utilize radiation spectra which deviate from the solar spectrum, especially in the photorepair wavelengths of ultraviolet-A radiation (UVAR: 321-399 nm) (Van Baalen and O'Donnell, 1972; Bornman, 1989). Unnatural radiation spectra have been avoided in some studies by utilizing natural sunlight (Jokiel and York, 1984; Behrenfeld et al., 1992).

A characteristic common to all previous studies of chronic UVBR effects on phytoplankton μ_{obs} and biomass has been the use of culture medium which is either naturally or artificially nutrient-replete (i.e., μ_{obs} is not limited by nutrients and is approximately equal to the intrinsic maximum growth rate (μ_{max})). Measured UVBR inhibition of nutrient-replete phytoplankton cultures may, at best, simulate effects of solar UVBR on oceanic phytoplankton in regions of high nutrient concentration, such as during the onset of coastal blooms at mid-latitudes. However, in most open ocean regions macro- or micro-nutrients are at concentrations low enough to limit phytoplankton biomass and perhaps μ_{obs} (Martin et al., 1991; Falkowski and Woodhead, 1992). Effects of UVBR on nutrient-replete phytoplankton cultures may not be representative in these low nutrient regions.

Research on environmental factors controlling growth rates of agricultural plants led Liebig (1840) to the conclusion that growth rate of a plant is determined by the nutrient which is present in the most limiting quantity (commonly referred to as Liebig's "law" of the minimum). We measured the effects of UVBR on μ_{obs} and biomass of nutrient-replete, carbon-limited, and nitrate-limited monocultures of the temperate marine diatom *Phaeodactylum tricornutum*. Photoinhibition of μ_{obs} and biomass by UVBR in *P. tricornutum* was only measurable under nutrient-replete conditions, when

UVBR stress was the most limiting factor. No effect of UVBR was detectable when μ_{obs} and biomass were limited to a greater extent by nutrient stress than by UVBR stress. Results suggest that interactions between UVBR and nutrient stress follow Liebig's "law" of the minimum and that nutritional status of an ecosystem should be considered when evaluating the potential effect of increased UVBR on phytoplankton populations.

MATERIALS AND METHODS

Nutrient-limited continuous cultures

Cultures of the temperate marine diatom *Phaeodactylum tricornutum* Bohlin (NEPCC Clone 31) were grown on a 12h:12h light:dark cycle at 15°C in an environmental growth chamber (Environmental Growth Chambers Model GC-15). Cultures were allowed to acclimate to the light:dark cycle for >130 hrs prior to UVBR exposure. *P. tricornutum* was chosen as the test organism because it is chronically sensitive to UVBR (Jokiel and York, 1984; Behrenfeld et al., 1992), even in the presence of high UVAR intensities.

Phaeodactylum tricornutum was grown in 2 L vessels constructed of quartz or Pyrex^R tubing with Pyrex^R watch glass bottoms and non-toxic silicone stopper tops. Phytoplankton were maintained in suspension by gentle stirring. Phytoplankton cultures were initially grown using f/2 growth medium (Guillard and Ryther, 1962) prepared using artificial seawater (32 $^0/_{00}$ salinity) (Kester et al., 1967; Davey et al., 1970) and then nutrient-limited (carbon or nitrate) prior to UVBR exposure using growth medium containing 84 µM carbon as bicarbonate or 5 µM nitrate as $NaNO_3$. Vitamins, trace metals, and nutrients other than the limiting nutrient were added at f/2 concentrations. Stock

medium was delivered to each culture through non-toxic silicone tubing at a rate of 1 L d^{-1}.

Cell concentrations and cell volumes were measured each day at the end of the light period, UVBR exposure period, and dark period using an electronic particle counter (El-Zone Model 80XY) calibrated using standardized latex microspheres traceable to the National Institute of Standards and Technology. Triplicate counts were made for each culture vessel during each sampling period (s.d. $\leq$ 2% of total count). Cell concentrations were used to calculate daily specific growth rates (μ_{obs}) as:

$$\mu_{obs} = \left(\frac{\ln (N_1/N_0)}{t_1 - t_0} \right) + D$$

where: t_1 is the time (hrs) of sampling, t_0 is time (hrs) of previous sampling, N_0 and N_1 are cell concentrations at t_0 and t_1, respectively, and D is the dilution rate (i.e., 0.5 d^{-1}). Biomass was calculated as cell concentration (cells ml^{-1}) * cell volume (μm^3 $cell^{-1}$). Differences in μ_{obs} and biomass accumulation rates (ξ) between treatments were tested using methods outlined by Winer (1962) for multifactor-repeated measurement analysis.

Phytoplankton cells were periodically collected from each continuous culture vessel, filtered onto Whatman^R GF/F filters, and analyzed for particulate organic carbon and

nitrogen using a Perkin-Elmer 240C Elemental Analyzer calibrated with acetanilide and chlorodinitrobenzene. Filtrate from the particulate carbon and nitrogen samples was collected and analyzed for residual phosphate and nitrate using an Alpkem Rapid Flow Analyzer (Model RFA/2) calibrated using KH_2PO_4 and KNO_3 standards (precision ≈ 0.10%, accuracy > 95%).

UVBR treatments used during the experiment were: (1) UVBR excluded, (2) moderate UVBR representative of late spring intensities at 45° lat. (2133 J m^{-2} d^{-1} EXP_{300}; i.e., weighted by the exponential action spectrum of Behrenfeld et al. (1993 b) normalized to 1 at 300 nm), and (3) enhanced UVBR (6285 J m^{-2} d^{-1} EXP_{300}) to simulate ozone depletion conditions. For comparison, the current daily dose of clear sky solar UVBR at 45°N during late spring is approximately 3500 J m^{-2} d^{-1} EXP_{300}. Three replicate cultures were used for each treatment and were positioned randomly within the growth chamber. The UVBR excluded treatment was created by wrapping culture vessels with a sheet of Mylar^R film (315 nm cutoff). Pyrex^R glass, which transmits less UVBR than quartz, was wrapped with a sheet of cellulose acetate (290 nm cutoff filter) to provide the moderate UVBR treatment. The enhanced UVBR treatment was created using quartz vessels wrapped with cellulose acetate. Transmittance properties of cellulose acetate and Mylar^R photodegrade upon exposure to light and were therefore replaced each day prior to the

onset of the light period. Intensities of wavelengths >346 nm were identical for all three treatments.

Photosynthetically active radiation (PAR: 400-700 nm) was supplied by 20 VHO Daylight fluorescent lamps (Philips Lighting Comp. Model F72T12/D/VHO) pre-burned for approximately 100 hrs. Daylight fluorescent lamps produce a more uniform visible spectrum than standard fluorescent lamps and therefore better simulate the solar spectrum (Fig. 3-1). Incandescent 60 W bulbs were used to supplement the longer PAR wavelengths. An 18-step, 12-hr light period was used to simulate daily changes in solar PAR. Daily integrated PAR flux was 1.4 X 10^6 J m^{-2} d^{-1}, <20% of near-noon summer solar intensities at mid-latitudes. Reflective walls were used within the growth chamber to distribute light more evenly. However, a PAR gradient did exist such that culture vessels near the sides of the chamber received ≈16% less PAR than cultures positioned in the center. A similar gradient in UVAR and UVBR did not occur because these wavelengths were provided by separate lamps for each culture vessel.

Photorepair wavelengths of UVAR were supplied during a 7-hr period, centered around the PAR light cycle, using UV-A340 ultraviolet fluorescent lamps (National Biological Corp.) pre-burned for approximately 80 hrs. Each phytoplankton culture received a daily integrated UVAR dose of 2.2 X 10^5 J m^{-2} d^{-1} at a rate of 31,508 J m^{-2} hr^{-1} (<20% near-noon summer solar intensity) (Fig. 3-1).

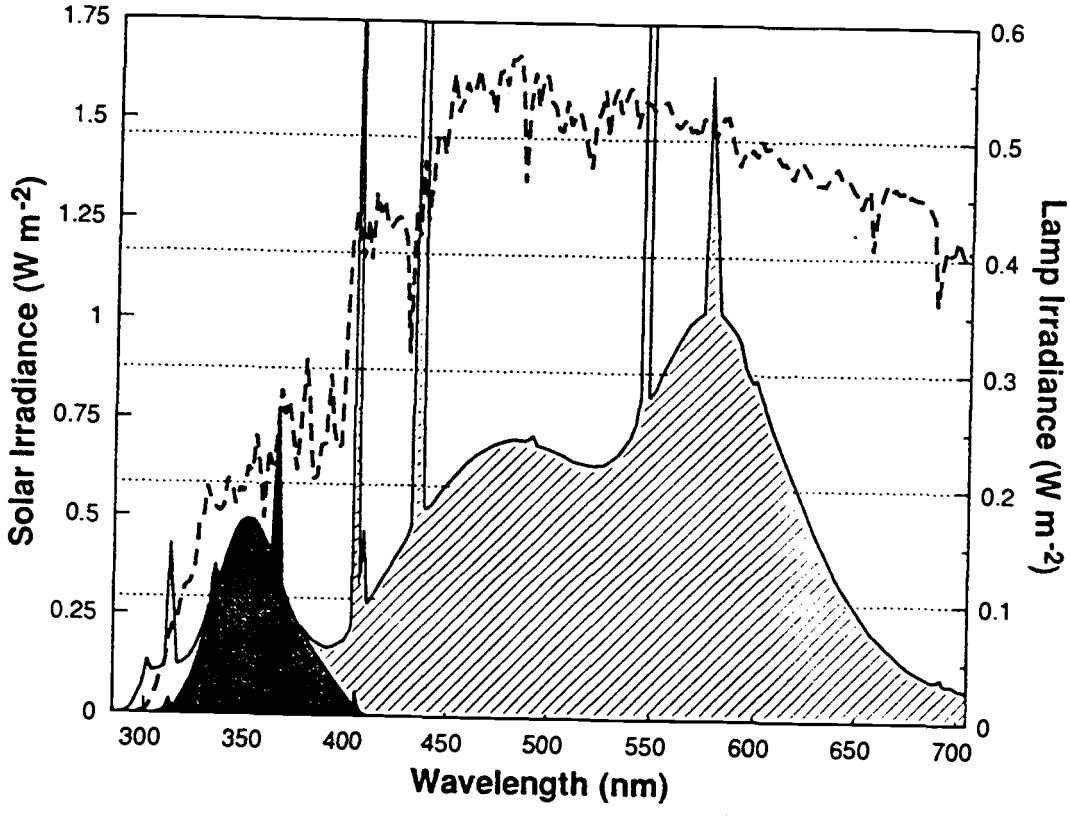

Figure 3-1. Solar spectrum and lamp spectrum used during the experiment (note different axis for solar and lamp irradiance). – – = Near-noon solar spectrum under clear skies at 45°N; —— = Additive spectrum of all lamps; Dark stipple = UV-A340 lamp spectrum; /// = Daylight fluorescent lamp spectrum; UV-B313 lamp spectrum denoted by blank area under additive spectrum.

UVBR doses were provided during the center of the PAR cycle using UV-A340 (7 hrs) and UV-B313 (3 hrs) ultraviolet fluorescent lamps (National Biological Corp.) pre-burned for approximately 80 hrs. UVBR irradiance was <40% near-noon summer solar intensities. However, the spectrum of UV-B313 lamps is enriched in the short UVBR wavelengths and therefore represents a greater biologically effective UVBR dose than solar radiation. The biologically effective doses in the moderate and enhanced UVBR treatments, when weighted by the exponential action spectrum described in Chapter 1 normalized to 1 at 300 nm (i.e., EXP_{300}), were 2133 and 6285 J m^{-2} d^{-1} EXP_{300}, respectively. For comparison, the moderate and enhanced UVBR doses would also correspond to 1727 and 5405 J m^{-2} d^{-1} when weighted by the DNA action spectrum of Setlow (1974), 2320 and 5729 J m^{-2} d^{-1} when weighted by the Caldwell Plant Action spectrum (Caldwell, 1971), and 10,974 and 18,028 J m^{-2} d^{-1} when weighted by the Photoinhibition action spectrum (Jones and Kok, 1966).

UVBR, UVAR, and PAR intensities were measured using an Optronic Model 752 spectroradiometer. The spectroradiometer was calibrated for wavelength offset by scanning a mercury arc lamp, and for intensity using a constant current source and halogen lamp traceable to the National Institute of Standards and Technology (Optronic Laboratories, Inc.). The Optronic 752 spectroradiometer has a reported wavelength

accuracy of ±0.3 nm, precision of ±0.1 nm, and an intensity accuracy of ±2-4% for the wavelength range of 200-800 nm.

Nutrient-replete batch cultures

Effects of UVBR on nutrient-replete *P. tricornutum* were determined using batch cultures in "f/2" growth medium (Guillard and Ryther, 1962). Light cycles, UVBR and UVAR doses, and sampling procedures used during this nutrient-replete experiment were identical to those described above for the nutrient-limited continuous culture studies. Nutrient-replete (batch) UVBR exposures were continued until the end of exponential growth (≈130 hrs). Differences in cell volume between treatments were tested using methods for multifactor-repeated measurement analysis outlined by Winer (1962). Differences in division rates (μ_{obs}) during exponential growth between UVBR treatments were compared using the slope of the regression for the natural logarithm of cell concentration versus time. One of the UVBR excluded treatment cultures exhibited early contamination during the nutrient-replete study and therefore only two replicate UVBR excluded cultures were used for comparisons between treatments. Exclusion of this culture did not change our overall conclusions, but did cause observed differences between the UVBR excluded and moderate UVBR treatments to be less than significant.

RESULTS

Nutrient-replete cultures

Specific growth rate (μ_{obs}) of *P. tricornutum* under nutrient-replete conditions was greatest (0.92 d^{-1}; R^2 = 0.995) in the UVBR excluded treatment, representing the maximum intrinsic growth rate (μ_{max}) for the environmental conditions existing during the experiment (Fig. 3-2). The moderate UVBR dose (2133 J m^{-2} d^{-1} EXP_{300}) decreased μ_{obs} ($p<0.05$) to 0.90 d^{-1} (R^2 = 0.995) (Fig. 3-2). Enhancement of UVBR to 6285 J m^{-2} d^{-1} EXP_{300} further reduced μ_{obs} ($p<0.001$) to 0.79 d^{-1} (R^2 = 0.994) (Fig. 3-2). Inhibition of nutrient-replete *P. tricornutum* growth has also been reported by Jokiel and York (1984) and Behrenfeld et al. (1992). Behrenfeld et al. (1992) reported an increase in cell volume with increasing doses of UVBR. During the current study, no difference in cell volume (spherical equivalents) existed between UVBR treatments ($p > 0.10$) (mean cell volume for all treatments = 69.5 μm^3) (Fig. 3-3). Cell growth and division in all UVBR treatments were synchronized to the light:dark cycle, as indicated by an increase in cell volume during the light period (growth) and decrease during the dark period (division) (Fig. 3-3).

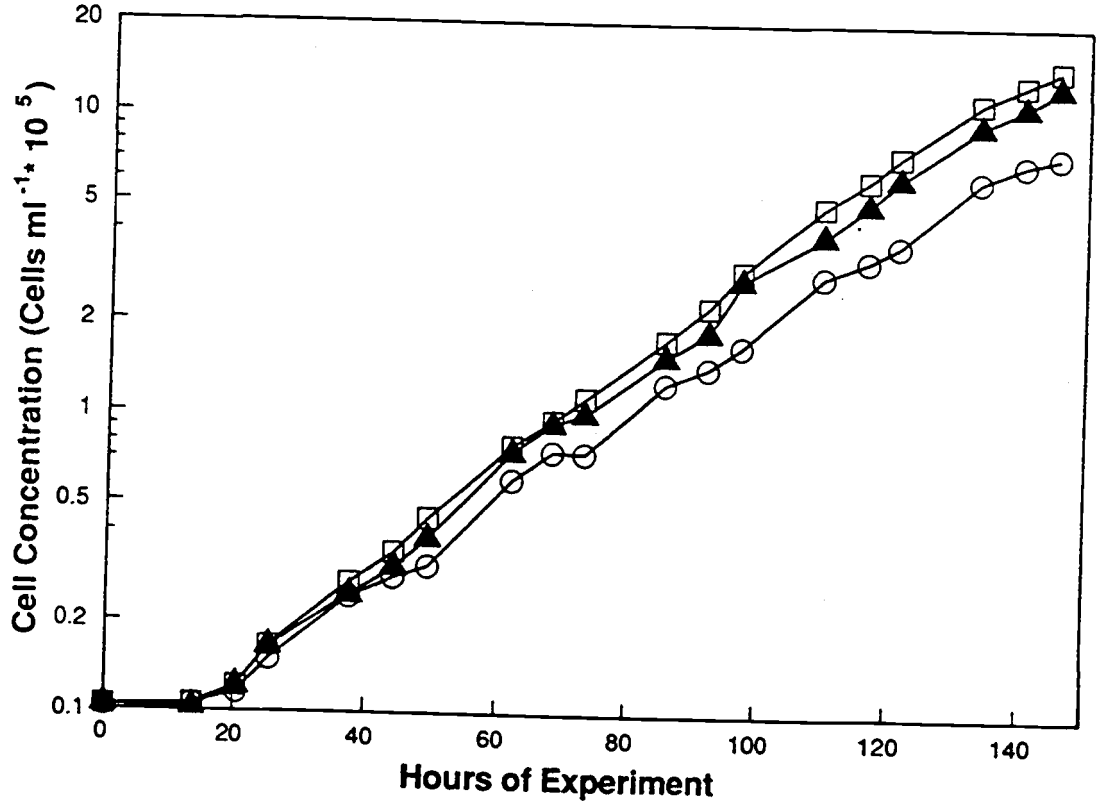

Figure 3-2. Mean cell concentrations (ml^{-1}) of *P. tricornutum* during nutrient-replete exponential growth. □ = UVBR excluded; ▲ = Moderate UVBR; O = Enhanced UVBR. Slope of growth curves indicates specific growth rate (μ_{obs}) for each UVBR treatment.

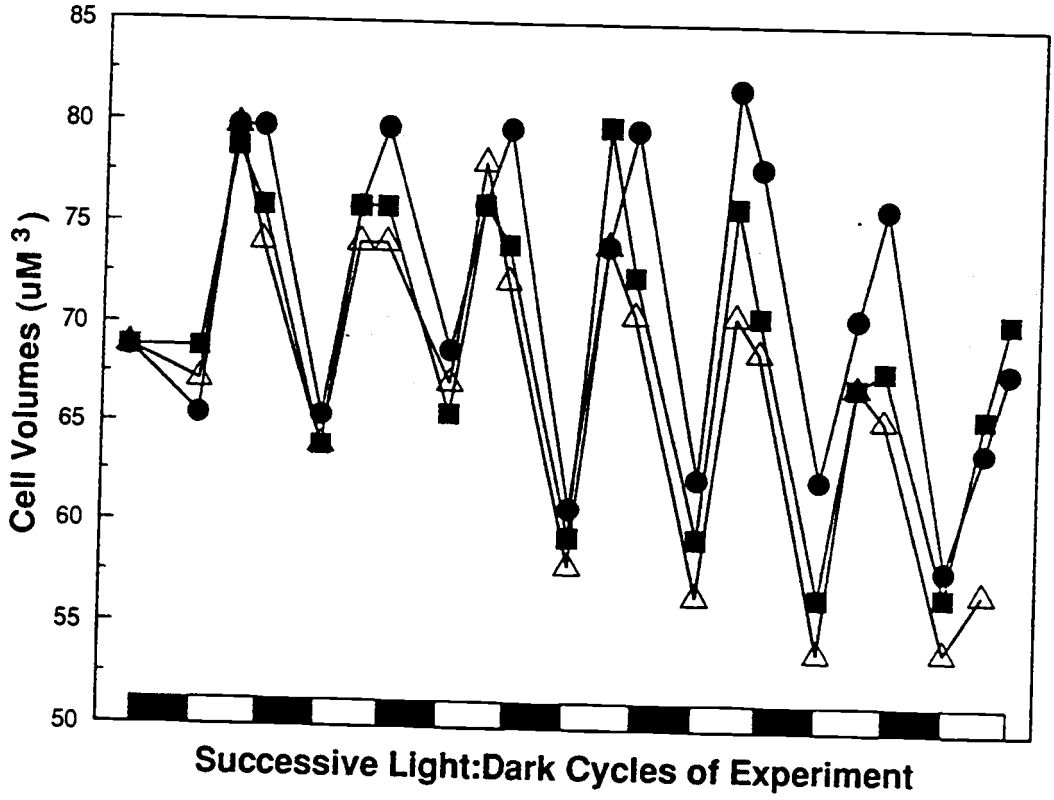

Figure 3-3. Changes in cell volumes of *P. tricornutum* during nutrient-replete growth during successive 12h:12h light dark cycles. ■ = UVBR excluded; ▲ = Moderate UVBR; ● = Enhanced UVBR.

Carbon-limited cultures

Cell concentrations in the carbon-limited cultures increased exponentially following inoculation and then stabilized after 140 hrs when the cells became carbon-limited (Fig. 3-4). UVBR exposures were started after 150 hrs. No significant differences in cell concentration (Fig. 3-4) or μ_{obs} occurred between UVBR treatments ($p > 0.10$). Carbon-limited μ_{obs} varied from 0.41 to 0.56 d^{-1}. Fluctuations in μ_{obs} were most highly correlated (s.d. ±2.1%) between the UVBR excluded and UVBR enhanced (6285 J m^{-2} d^{-1} EXP_{300}) treatments (Fig. 3-5). For comparison, this same dose of 6285 J m^{-2} d^{-1} EXP_{300} decreased μ_{obs} by 16% during the nutrient-replete study (Fig. 3-2). Thus, effects of UVBR on *P. tricornutum* μ_{obs} were not detectable when inhibition of μ_{obs} by carbon limitation exceeded the potential for inhibition by UVBR.

Mean cell volume remained low (60-70 μm^3) during the exponential growth period prior to UVBR exposure and then increased during carbon limitation to a final cell volume of 108 μm^3, with no significant difference between UVBR treatments ($p > 0.10$) (Fig. 3-6). Increases in cell volume (Fig. 3-6) were correlated to slight decreases in cell concentration (Fig. 3-4), resulting in a constant biomass concentration (Fig. 3-7a). Cell concentrations were

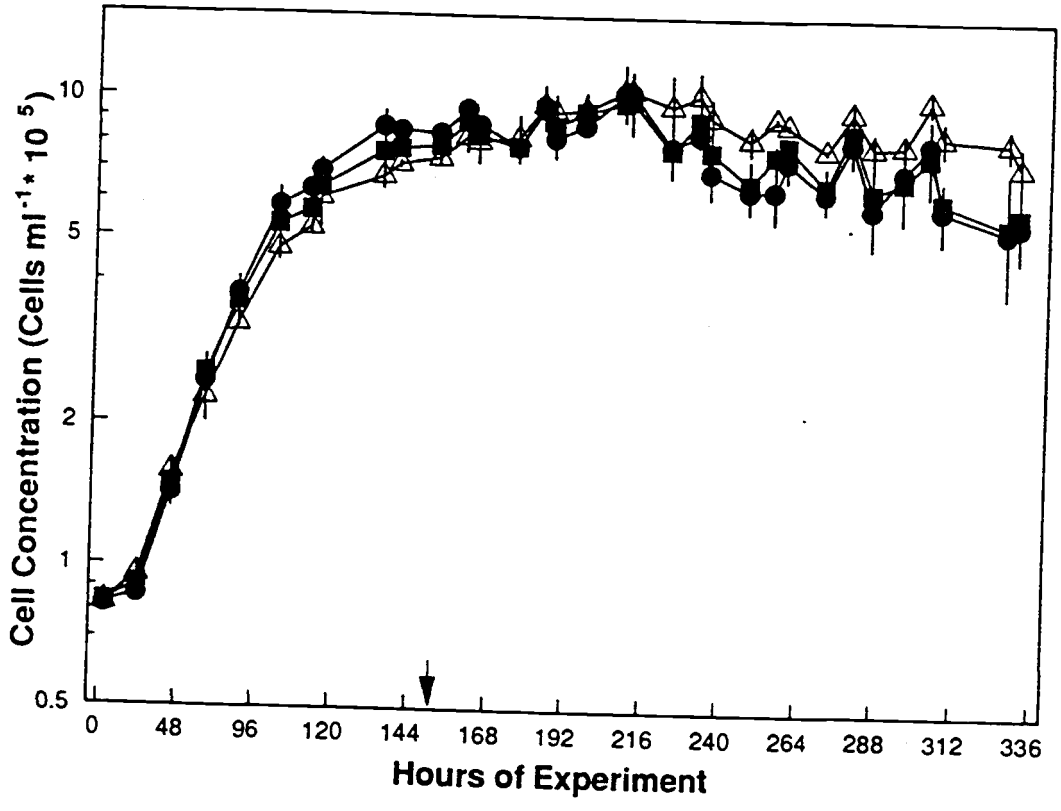

Figure 3-4. Mean cell concentrations during carbon-limited growth of *P. tricornutum*. Error bars indicate standard deviations. UVBR exposure was initiated at 150 hrs, as indicated by arrow. ■ = UVBR excluded; ▲ = Moderate UVBR; ● = Enhanced UVBR.

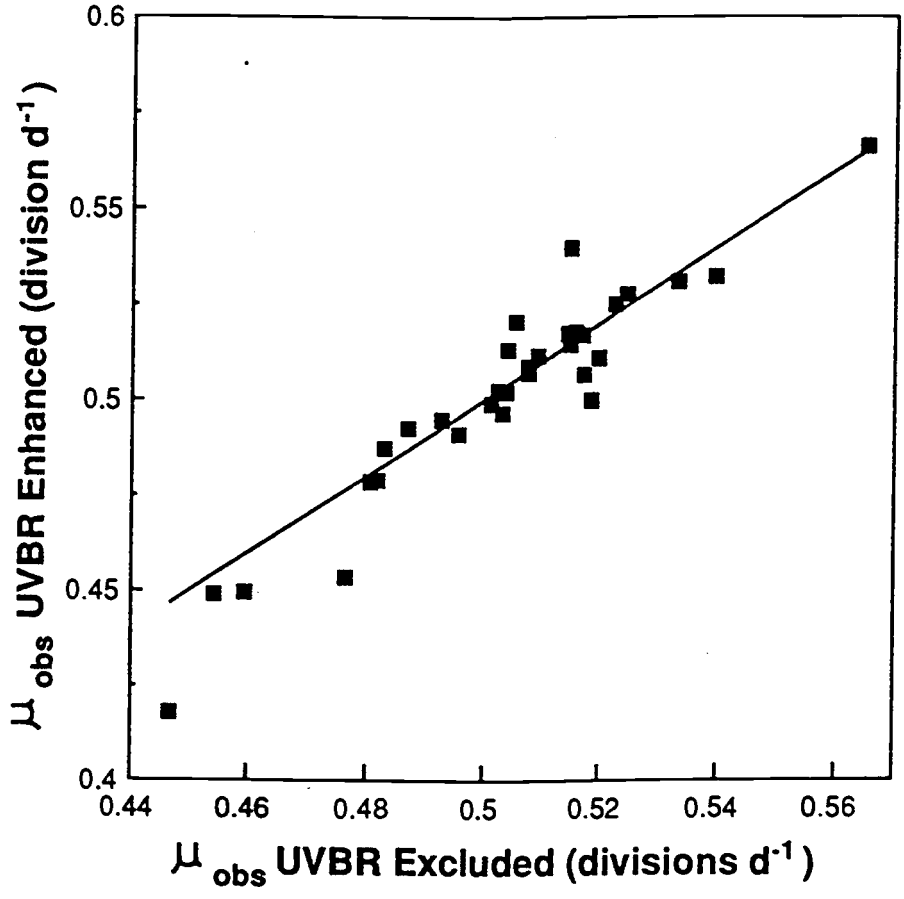

Figure 3-5. Carbon-limited μ_{obs} (divisions d^{-1}) of *P. tricornutum* in the UVBR excluded versus enhanced UVBR treatments. Solid line indicates an exact 1:1 correlation between μ_{obs}.

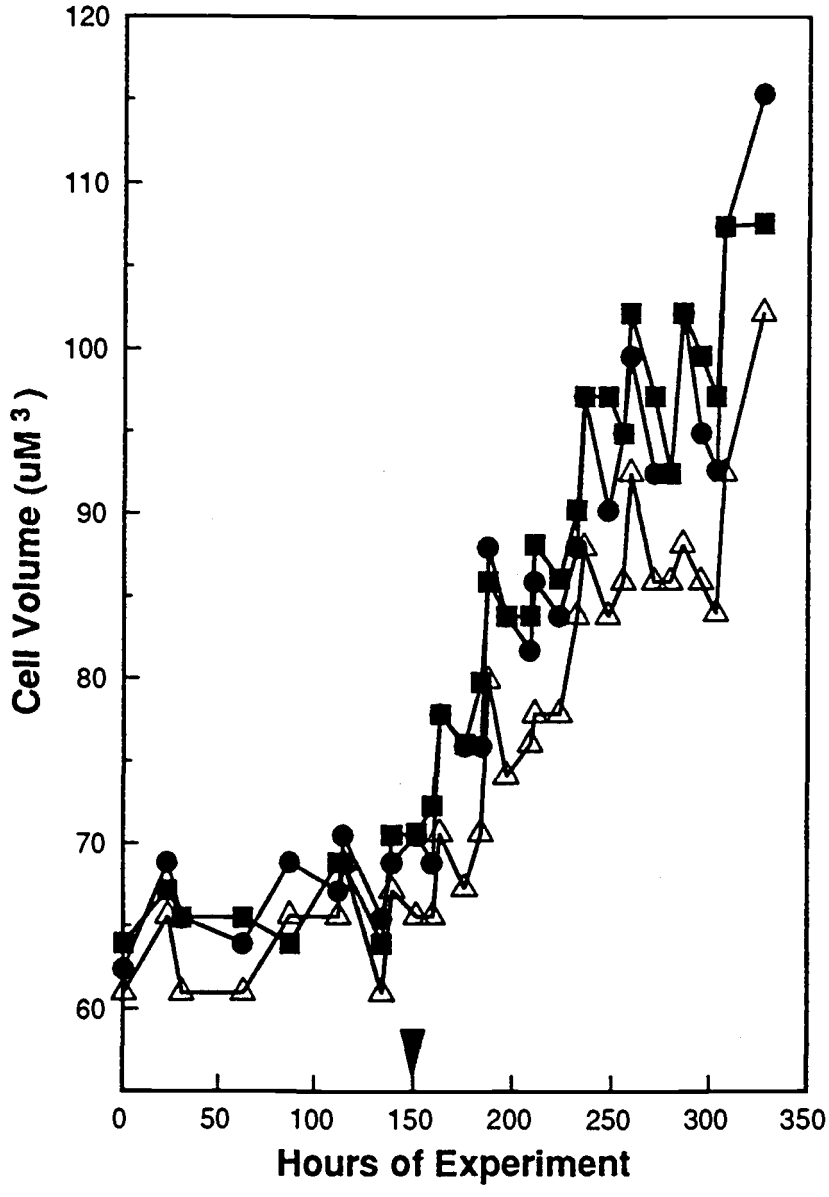

Figure 3-6. Mean cell volume of *P. tricornutum* during carbon-limited growth. Initiation of UVBR exposure indicated by arrow. ■ = UVBR excluded; ▲ = Moderate UVBR; ● = Enhanced UVBR.

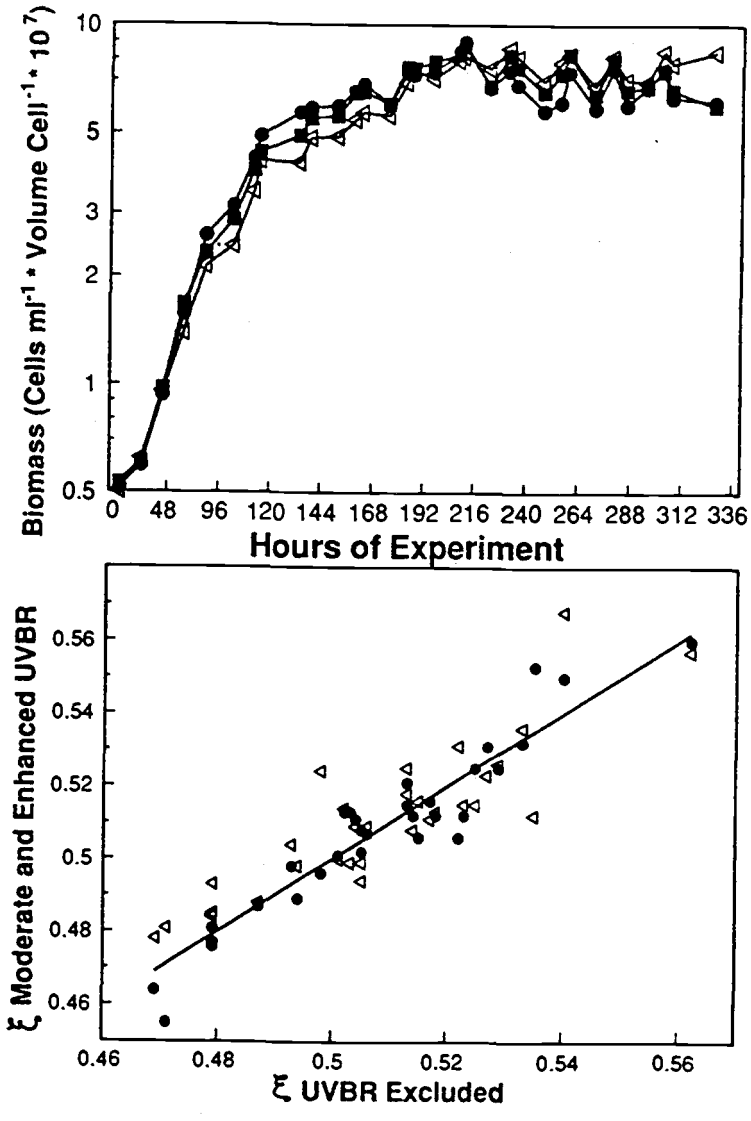

Figure 3-7. (a) Biomass standing stock and (b) biomass accumulation rates (ξ: μm^3 ml^{-1} d^{-1}) of carbon-limited *P. tricornutum* in all UVBR treatments. ■ = UVBR excluded; ▲ = Moderate UVBR; ● = Enhanced UVBR. Solid line in (b) indicates an exact 1:1 correlation between treatments.

slightly higher (Fig. 3-4) and cell volume were slightly lower (Fig. 3-6) in the moderate UVBR treatment (2133 J m^{-2} d^{-1} EXP_{300}) than the other UVBR treatments. Thus, ξ had a greater correlation between all UVBR treatments than μ_{obs} (Fig. 3-7b).

No difference in particulate organic carbon (mean = 14.4 pg μm^{-3}) or nitrogen (mean = 2.5 pg μm^{-3}) occurred between UVBR treatments ($p>>0.10$) (mean C:N ratio = 5.8). Replete concentrations of nitrate (mean = 598 μM) and phosphate (mean = 20 μM) persisted throughout the UVBR exposure period. As a final check for carbon limitation, the experiment was repeated using one culture bubbled with CO_2 and three cultures without CO_2 bubbling (data not shown). Cultures without additional carbon became limited at $\approx 7.7 * 10^5$ cells ml^{-1} while the culture with additional CO_2 continued to grow exponentially to $3.3 * 10^6$ cells ml^{-1}, at which time the experiment was terminated.

Nitrate-limited cultures

Phaeodactylum tricornutum grew exponentially during the first 80 hrs of the nitrate-limited study. Within 100 hrs, nitrate concentrations were depleted to <1 μM and cell concentrations stabilized (Fig. 3-8). Phosphate, vitamins, and trace metals remained at replete concentrations throughout the experiment. UVBR exposure was started after

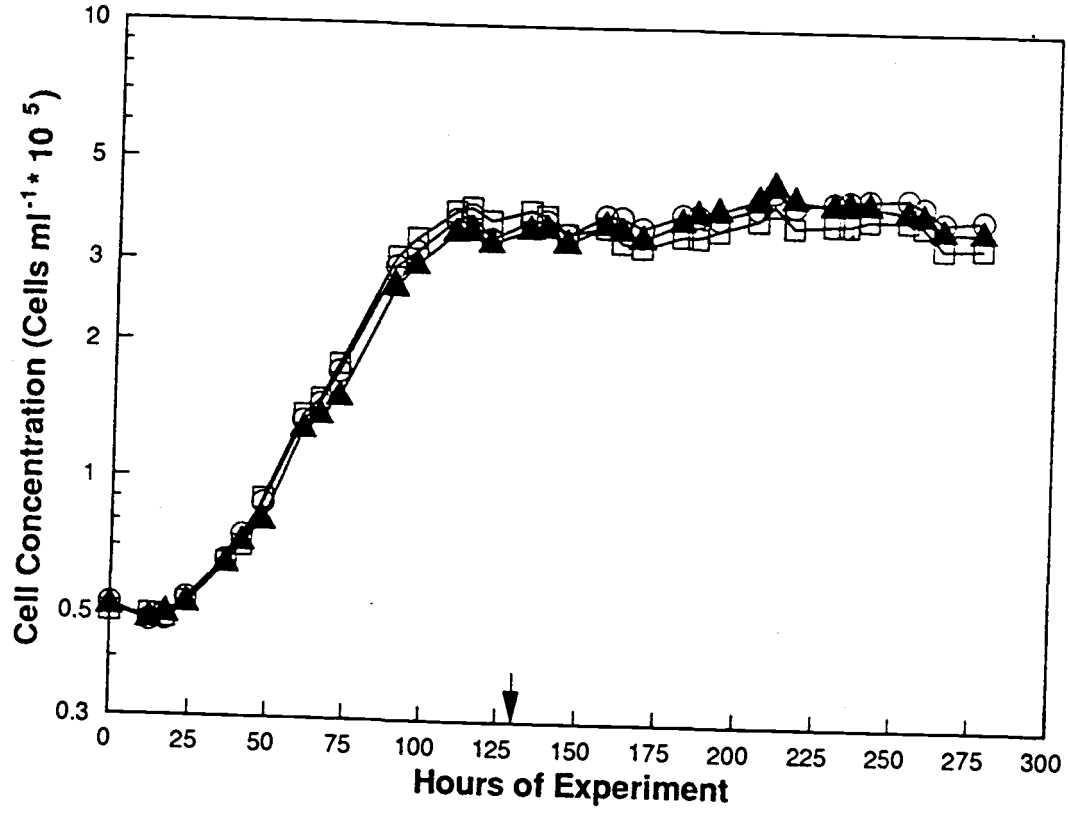

Figure 3-8. Mean cell concentrations during nitrate-limited growth of *P. tricornutum*. UVBR exposure was initiated at 132 hrs, as indicated by arrow. O = UVBR excluded; ▲ = Moderate UVBR; □ = Enhanced UVBR.

132 hrs. As in the carbon-limited study, no significant differences ($p > 0.10$) in cell concentration (Fig. 3-8) or μ_{obs} (Fig. 3-9) occurred between treatments after initiation of UVBR exposure. Nitrate-limited growth rates were less variable (0.48 and 0.52 d^{-1}) than during the carbon-limited study and were highly correlated between all UVBR treatments (Fig. 3-9). Mean cell volume fluctuated between 30 and 42 μm^3, with no significant overall differences between UVBR treatments ($p > 0.10$) (Fig. 3-10). However, mean cell volume was slightly higher (Fig. 3-10) and cell concentrations slightly lower (Fig. 3-8) in the enhanced UVBR treatment during the final 70 hrs of the experiment. Thus, biomass (cell concentration * cell volume) had a greater correlation between UVBR treatments than μ_{obs} (Fig. 3-11).

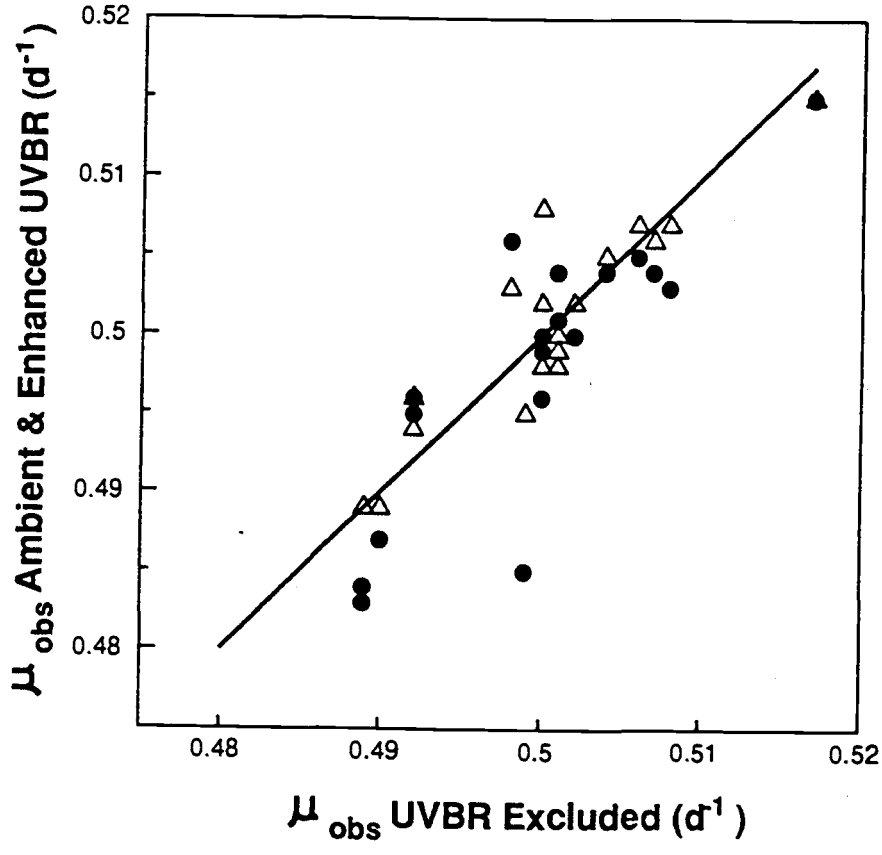

Figure 3-9. Mean μ_{obs} (divisions d^{-1}) in the moderate and enhanced UVBR treatments versus μ_{obs} in the UVBR excluded treatment during nitrate-limited growth. Solid line indicates an exact 1:1 correlation between treatments. △ = Moderate UVBR; ● = Enhanced UVBR.

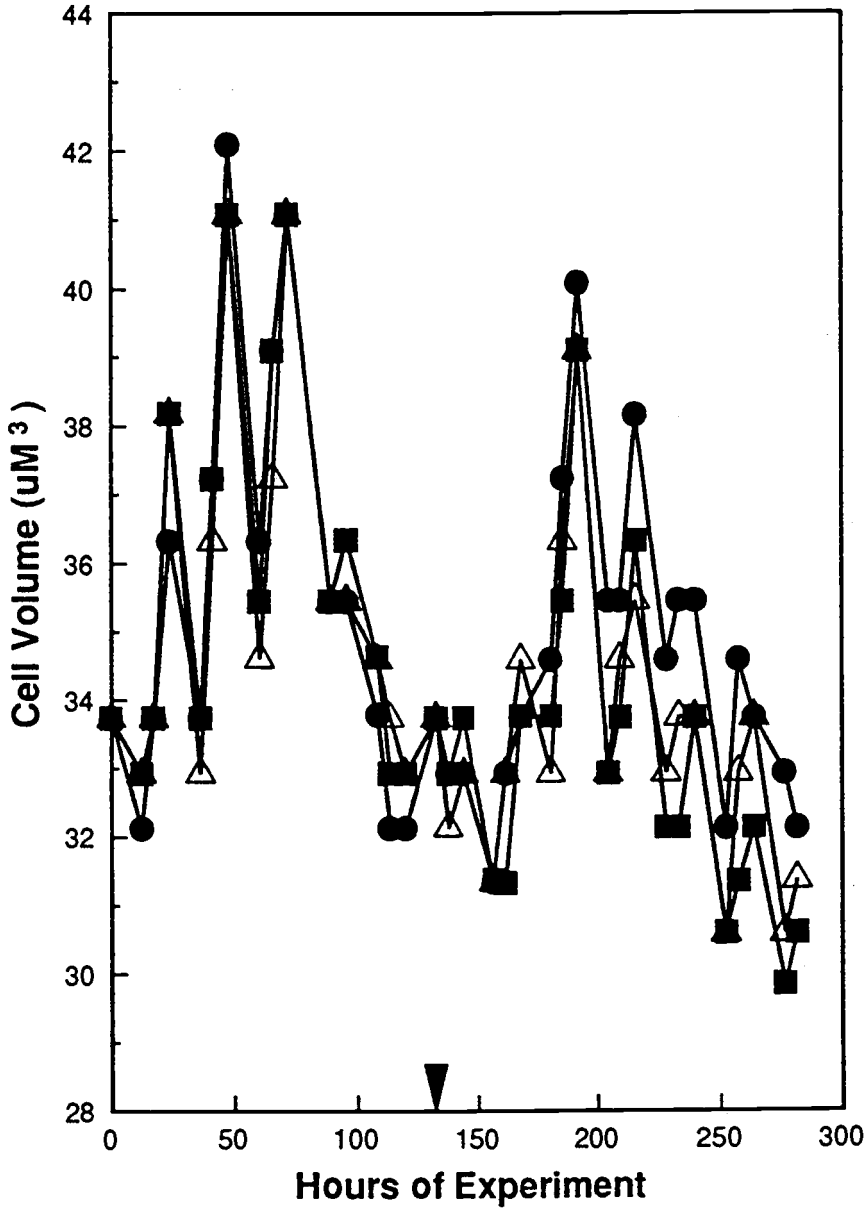

Figure 3-10. Mean cell volume of *P. tricornutum* during nitrate-limited growth. Initiation of UVBR exposure indicated by arrow. ■ = UVBR excluded; ▲ = Moderate UVBR; ● = Enhanced UVBR.

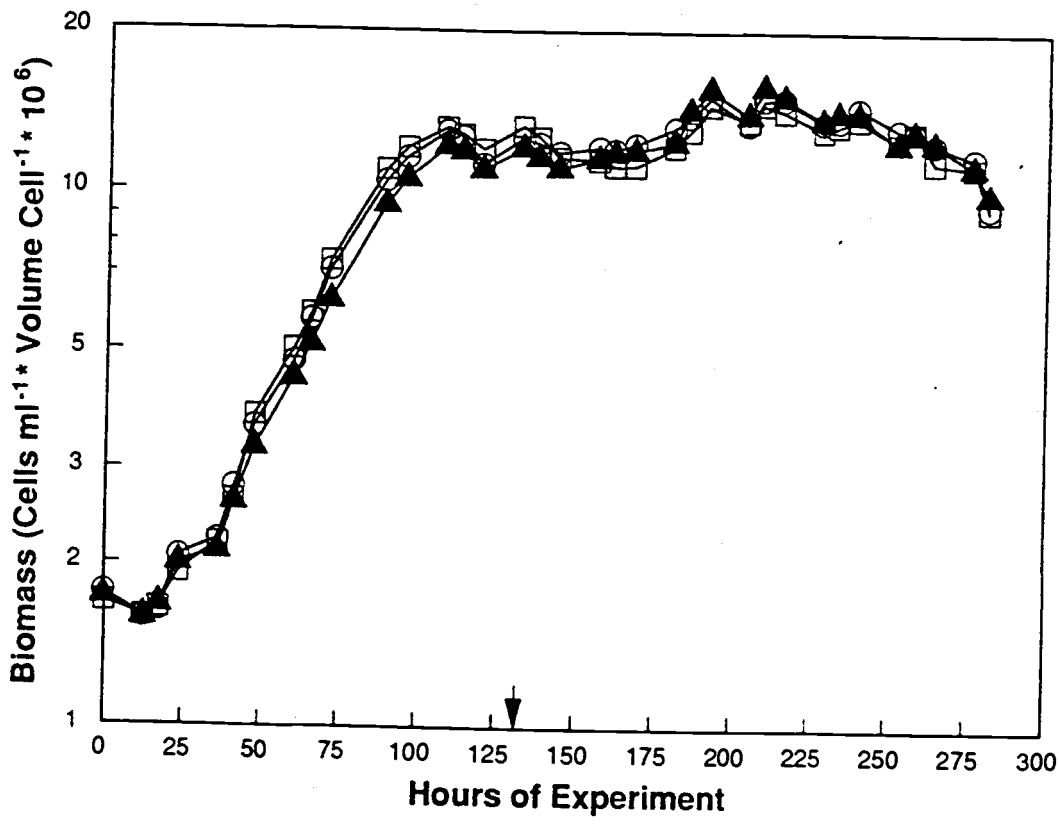

Figure 3-11. Biomass standing stock (μm^3 ml^{-1}) of nitrate-limited *P. tricornutum*. O = UVBR excluded; ▲ = Moderate UVBR; □ = Enhanced UVBR.

DISCUSSION

Growth inhibition of *P. tricornutum* by UVBR was first discovered by Jokiel and York (1984). Behrenfeld et al. (1992) found UVBR inhibition of *P. tricornutum* growth to be persistent during 36 days of UVBR exposure. Growth inhibition of *P. tricornutum* by UVBR was also noted by Ekelund (1990). These studies used nutrient-replete culturing methods. UVBR photoinhibition of μ_{obs} and ξ in nutrient-replete *P. tricornutum* cultures measured during the current study is consistent with results of these earlier studies and confirms that the lack of UVBR effect observed during nutrient-limited conditions was not due to errors in experimental design.

No effect of UVBR was observed on μ_{obs} or ξ of nutrient-limited *P. tricornutum*. It is unlikely that nutrient limitation stimulates UVBR adaptation in *P. tricornutum*. In the absence of UVBR, carbon- and nitrate-limited μ_{obs} were <60% of μ_{max} observed under nutrient-replete conditions (i.e., μ_{obs} was inhibited by >40% of μ_{max} by nutrient limitation). The decrease in μ_{obs} expected for a UVBR dose of 6285 J m^{-2} d^{-1} EXP_{300}, as measured during the nutrient-replete study, was 16%. Thus, when μ_{obs} and biomass were limited to a greater extent by nutrient stress than by UVBR stress, effects of UVBR were not measurable.

Our results indicate that a competitive interaction exists between UVBR and macro-nutrient stress on phytoplankton growth and biomass. Competitive interaction between stresses follows Liebig's (1840) "law" of the minimum, such that growth rate and biomass are determined by the most limiting factor. Additive or complementary interactions may also exist between UVBR and other growth factors. For example, photoinhibition by UVBR and high intensities of PAR may be additive, since both types of stresses are similar. A complementary interaction may exist between UVBR and iron-limitation. Palenik et al. (1991) suggested that phytoplankton productivity could, theoretically, be stimulated by UVBR in iron-limited regions of the ocean due to increased bioavailability of iron resulting from photochemical reactions between iron-containing colloids and UVBR.

Our study utilized a single phytoplankton species. Additional species should be tested before results are extrapolated to more complex systems. If biomass and division rate of natural phytoplankton exposed to UVBR respond in a manner similar to *P. tricornutum*, then our results should provide insight toward oceanic regions most susceptible to the adverse effects of increased UVBR. Measured UVBR inhibition of nutrient-replete phytoplankton growth and biomass may be representative of oceanic conditions which are temporally and spatially limited, such

as spring blooms at mid-latitudes. Absence of a measurable UVBR effect on nutrient-limited *P. tricornutum* suggest that, if growth rates and biomass of phytoplankton in oligotrophic regions of the ocean are limited by nutrients, then effects of UVBR may not be apparent. However, natural assemblages of phytoplankton contain both UVBR tolerant and UVBR sensitive species (Worrest et al., 1978; Bothwell et al., 1993). UVBR stress on sensitive phytoplankton species may decrease their competitive fitness and provide an advantage for less UVBR sensitive species, resulting in an alteration of community species composition.

CONCLUDING PERSPECTIVES

Models of surface photoinhibition of phytoplankton productivity by UVBR should be based on experimental results using natural phytoplankton communities. However, experimental artifacts resulting from long-term, open ocean growth studies have limited most UVBR effects studies on natural phytoplankton populations to short-term carbon uptake measurements. Comparison of dose-responses for short-term UVBR inhibition of carbon uptake in natural phytoplankton populations typically indicates a greater inhibitory effect of UVBR than longer-term laboratory growth studies using phytoplankton monocultures. Thus, models of UVBR effects on marine phytoplankton based on the dose-response and action spectrum for inhibition of carbon uptake likely represent the upper limit for ozone depletion effects.

Initial attempts to describe UVBR inhibition of phytoplankton carbon uptake (Smith et al., 1980) resulted in a linear dose-response model based on an action spectrum with relatively low wavelength dependence. However, uncertainty toward the representativeness of treatment spectra used during the study by Smith et al. (1980) has resulted in a re-evaluation of their response data and the description of a new dose-response and action spectrum for UVBR inhibition of phytoplankton carbon fixation (Chapter

1). The action spectrum chosen by Smith et al. (1980) for their dose-response model appears to have been strongly influenced by inclusion of UVCR wavelengths in their UVR-treatment spectra. The new exponential action spectrum for photoinhibition of carbon uptake by UVBR (Chapter 1) was determined from exposure studies utilizing UVR-treatments with all UVCR wavelengths excluded. The exponential action spectrum exhibits a steeper increase in biological damaging efficiency with decreasing UVBR wavelengths than the photoinhibition action spectrum (Jones and Kok, 1966) used by Smith et al. (1980). Photoinhibition of phytoplankton carbon uptake was found to be a linear function of cumulative UVBR dose weighted by the exponential action spectrum.

Inhibition of carbon fixation by UVBR in monocultures of the marine diatom *Thalassiosira pseudonana* was recently described by Cullen and Lesser (1991) as a function of dose-rate rather than total dose. Cullen et al. (1992) subsequently reported a dose-rate dependent action spectrum for UVBR photoinhibition. Dose-rate dependent responses of Cullen and Lesser (1991) and Cullen et al. (1992) differ from responses measured during the open ocean studies (Chapter 1), which appear independent of dose-rate. Description of photoinhibition of carbon fixation as a function of total UVBR dose (Chapter 1) indicates that reciprocity holds (i.e., the response is dose dependent and

dose-rate independent) within the range of UVBR doses used during the experiments; while the dose-rate dependence described by Cullen and Lesser (1991) indicates a failure of reciprocity. Results of the open ocean studies (Chapter 1) can be tested for reciprocity by comparing percent decreases per unit UVBR dose to dose-rate. To make this comparison, dose-rate must be expressed as an average for the ambient-UVBR treatment, while dose-rate in the UVBR-enhanced treatment can be calculated exactly due to the constant output of the ultraviolet fluorescent lamps. If reciprocity holds, the regression slope for the comparison of percent decrease per unit dose versus dose-rate will be zero. Reciprocity fails if the regression slope is either positive or negative. The test for reciprocity in the open ocean response data (Fig. 4-1) provides strong evidence that the measured inhibition of carbon fixation by UVBR was independent of dose-rate ($p<<0.001$). Variance in the reciprocity test (Fig. 4-1) is greatest for the ambient-UVBR responses because the ambient solar dose is an integrated average calculated from solar scan data collected at 17 minute intervals (i.e., the time required for a spectral scan between 280-800 nm using an Optronic model 752 spectroradiometer).

Measured UVBR inhibition of carbon uptake in *Thalassiosira pseudonana* (Cullen and Lesser, 1991) also indicated decreasing photoinhibitory efficiency with

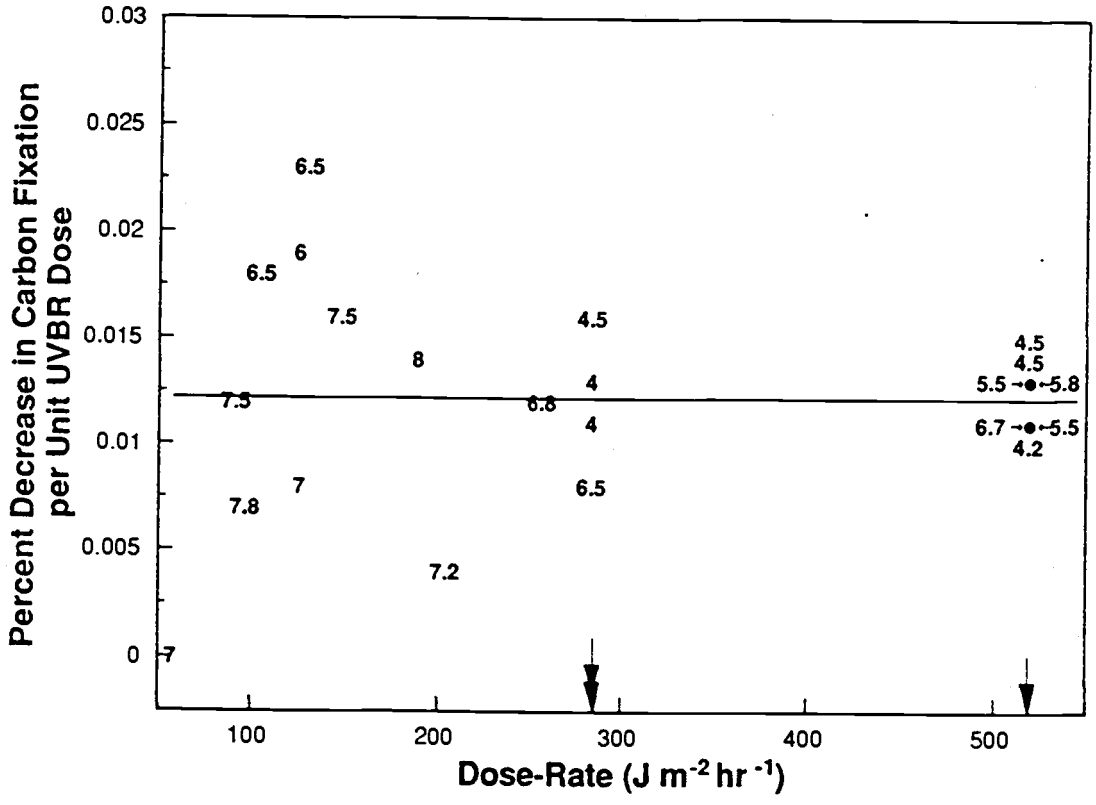

Figure 4-1. Test for reciprocity in the dose-response data for UVBR inhibition of photosynthetic carbon uptake. Dose-rate is total UVBR dose weighted by the exponential action spectrum divided by time of treatment. Observations are plotted using duration of treatment in hours. Solid line is regression for all data. Data corresponding to the UVBR enhanced treatment occur above the arrows. Single arrow = one screen over lamps. Double arrow = two screens over lamps.

increasing dose-rate (a curvilinear relationship). A similar decrease in the photoinhibition-rate with increasing UVBR dose-rate for the open ocean response data (Chapter 1) can be tested by comparing percent decrease per unit time to dose-rate. The resultant linear relationship (R^2 = 0.72) (Fig. 4-2) from this comparison provides evidence that photoinhibition-rate was independent of dose-rate for the range of UVBR dose-rates used during the experiments. Thus, photoinhibition of carbon fixation by UVBR measured during exposure experiments utilizing solar radiation spectra and natural phytoplankton assemblages from a range of oceanic regions is different from the results of Cullen and Lesser (1991) and Cullen et al (1992) for phytoplankton monocultures exposed to artificial radiation spectra.

The dose-response and action spectrum determined for UVBR inhibition of carbon fixation could be applied to predicted increases in surface UVBR to estimate the increase in surface photoinhibition resulting from stratospheric ozone depletion. A similar model using the dose-response and action spectrum for a metabolic process other than carbon fixation could also be created and may result in a different estimate of increased surface photoinhibition. Measurements of UVBR inhibition of nitrogen uptake (Chapter 2) provide a dose-response and action spectrum with which the carbon uptake results can be compared. Results of the

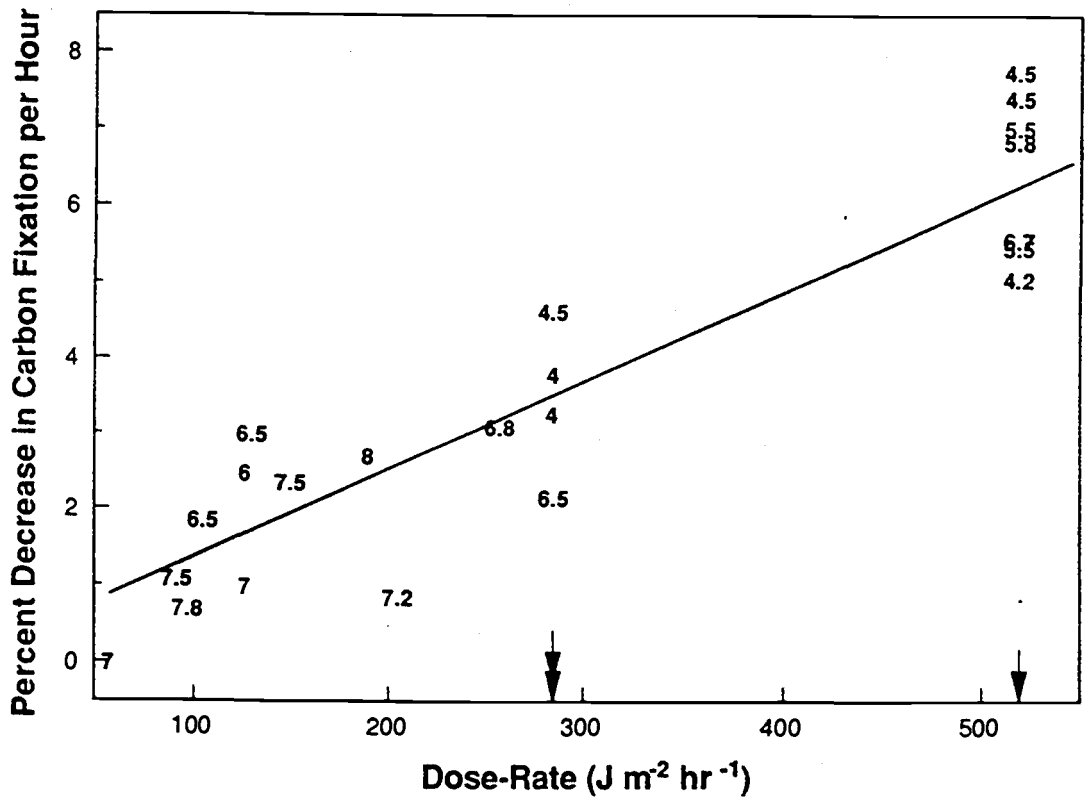

Figure 4-2. Test of photoinhibition-rate for UVBR inhibition of carbon fixation as a function of dose-rate. Dose-rate is total UVBR dose weighted by the exponential action spectrum divided by time of treatment. Observations are plotted using duration of treatment in hours. Solid line is regression for all data. Data corresponding to the UVBR enhanced treatment occur above the arrows. Single arrow = one screen over lamps. Double arrow = two screens over lamps.

nitrogen uptake experiments indicate a dissimilar effect of UVBR on nitrate and ammonium uptake (Chapter 2). Slopes of the dose-response and action spectrum for UVBR inhibition of ammonium uptake were lower than those for carbon uptake. Differences between the action spectra and dose-responses for UVR inhibition of carbon (Chapter 1) and ammonium uptake (Chapter 2) can be illustrated by comparing the estimated surface photoinhibition resulting from a modeled solar UVR increase. For this comparison, a model by Green et al. (1980) was used to calculate the diel changes in UVR (290-330 nm) resulting from a 16% decrease in ozone column thickness from 0.320 to 0.269 cm at 45°N on June 27th under clear skies. These conditions were chosen to allow comparison between modeled and measured UVR. Modeled UVR for an ozone column thickness of 0.320 cm was similar to clear-sky UVR measured with an Optronic model 752 spectroradiometer on June 27th, 1992 at Newport, Oregon (44° 37'N, 124° 03'W) (Fig. 4-3).

Increases in UVR energy from the modeled 16% decrease in ozone column thickness were greatest during mid-day (Fig. 4-3). Spectral maximum of the increased UVR (unweighted) shifted from 318 nm at 0600 hrs to 311 nm at 1200 hrs (not illustrated). Diel shifts in the spectral maxima are due to the wavelength dependency of atmospheric UVR attenuation, which increases with decreasing wavelength. Thus, the shortest UVBR wavelengths only contribute significantly to

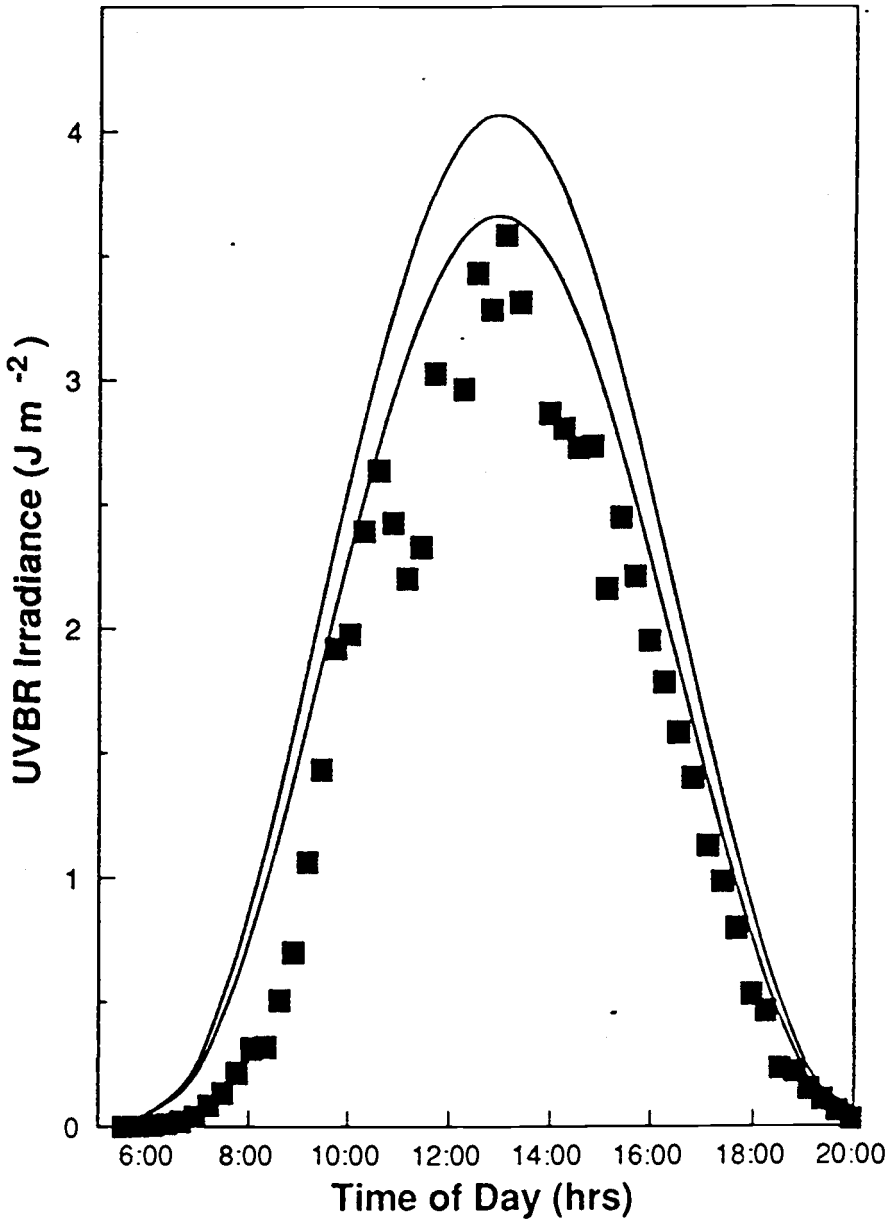

Figure 4-3. Wavelength integrated, unweighted solar UVR between 290-330 nm as measured at 44° 37'N (■) and modeled (Green et al 1980) for an ozone column thickness of 0.320 cm (lower solid curve) and 0.269 cm (upper solid curve).

the modeled increase during mid-day. Weighting the modeled increase in UVR by the action spectrum for ammonium uptake results in a daily biologically effective dose which 1) has spectral maxima between 307 and 315 nm, 2) is dominated by wavelengths >300 nm, and 3) exhibits a broad distribution having significant contributions to total dose from early and late hours (Fig. 4-4). In contrast, weighting the modeled increase in UVR by the much steeper action spectrum for carbon fixation (Chapter 1) results in a daily biologically effective dose which 1) has spectral maxima between 302 and 310 nm, 2) is essentially limited to wavelengths <320 nm, and 3) is dominated by mid-day hours when the shortest wavelengths are present (Fig. 4-5).

Integrating the weighted UVBR irradiances from 0600-1800 hrs results in a cumulative biologically effective dose of 6677 J m^{-2} using the action spectrum for ammonium uptake (Fig. 4-4) and 2230 J m^{-2} using the action spectrum for carbon uptake (Fig. 4-5). These increases in biologically effective dose would correspond to an estimated 19% decrease in ammonium uptake (Chapter 2) and 24% decrease in carbon uptake (Chapter 1), respectively. The decrease in carbon fixation occurs at a higher rate (maximum ≈ 3.8% hr^{-1}) over a shorter period of time than the decrease in ammonium uptake, with a maximum rate of ≈2.6% hr^{-1}. Conditions used in this model comparison resulted in similar total decreases in surface carbon and NH_4^+ uptake. However, such

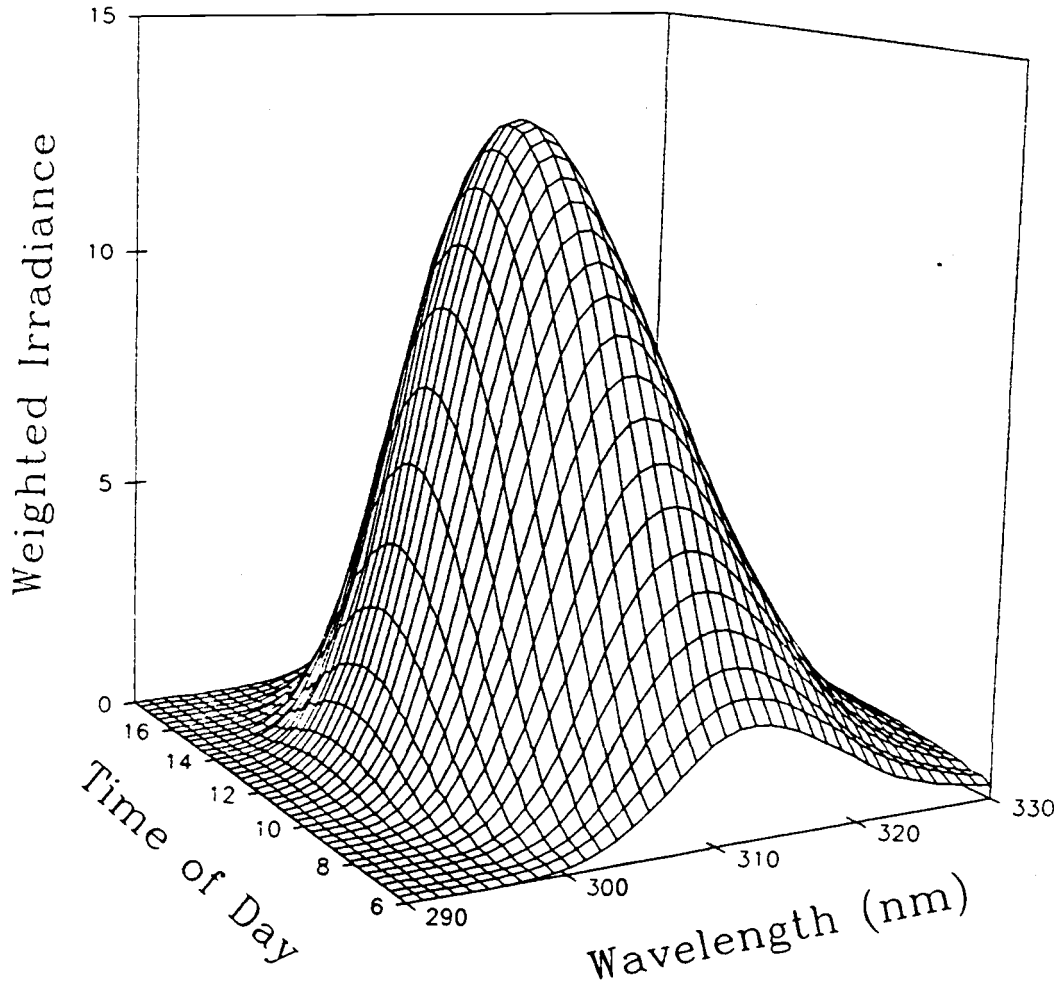

Figure 4-4. Wavelength specific, diel increase (0600-1800 hrs) in surface biologically effective ultraviolet radiation resulting from a modeled decrease in ozone column thickness of 16% (Green et al. 1980) weighted by the action spectrum for ρ_{NH4} inhibition (Chapter 2).

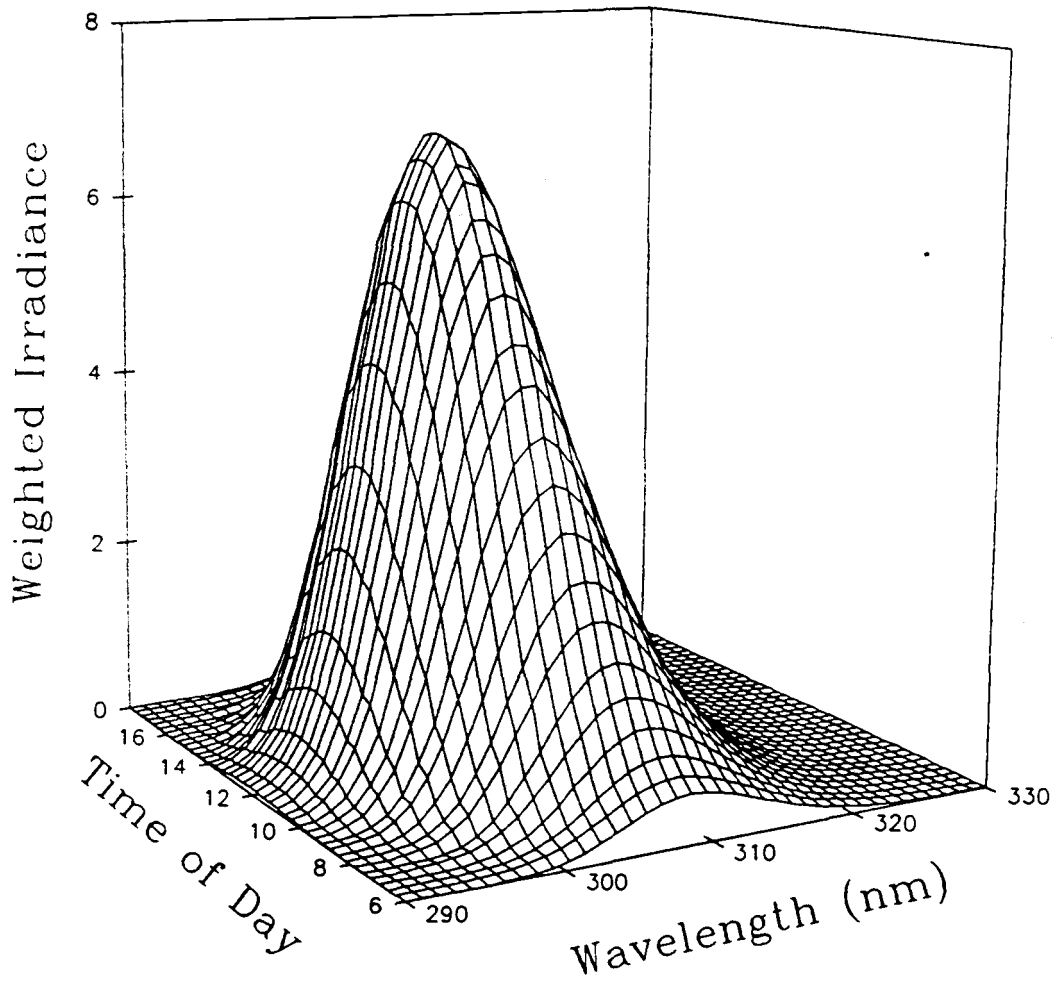

Figure 4-5. Wavelength specific, diel increase (0600-1800 hrs) in surface biologically effective ultraviolet radiation resulting from a modeled decrease in ozone column thickness of 16% (Green et al. 1980) weighted by the action spectrum for photoinhibition of carbon fixation (Chapter 1).

correlation may not occur with other spectral UVR increases or at different depths.

The modeled increase in solar UVR illustrates differences and similarities between the action spectra and dose-responses for UVBR inhibition of ammonium and carbon uptake. The estimated increase in surface photoinhibition, however, does not represent the effects of stratospheric ozone depletion on natural phytoplankton populations in the open ocean. The 16% decrease in stratospheric ozone used in the model is greater than expected at 45°N during mid-summer (Stolarski et al., 1992), thus the modeled increase in UVR is an overestimate. The model also does not account for influences of nutritional status of the cells on UVR inhibition (Cullen and Lesser 1991; Chapter 3). These and other factors must be considered with respect to a vertically mixing euphotic zone before credible estimates of ozone depletion effects can be made for marine phytoplankton production in the water column.

Depletions in stratospheric ozone concentrations increase with increasing latitude, while surface intensities of solar UVBR increase with decreasing latitude. This latitudinal relationship between ozone depletion and solar radiation results in the largest UVBR increases at mid-latitudes (30°-50°) and in Antarctica during the "ozone hole" events. Effects of increased UVBR from stratospheric ozone depletion modeled using the dose-response for carbon

uptake will result in a spatial pattern that mimics the increase in UVBR intensity (i.e., greatest in Antarctica and at mid-latitudes). However, vast oceanic regions at mid-latitudes are characterized by nutrient concentrations which are low enough to limit phytoplankton population growth. Measurements of UVBR inhibition on nutrient-limited phytoplankton (Chapter 3) indicate no change in phytoplankton biomass or cell division rate when these parameters of phytoplankton productivity are limited to a greater extent by nutrients than the UVBR dose. However, measurements of short-term carbon uptake in these low-nutrient regions (Chapter 1) indicate a significant decrease from UVBR exposure.

UVBR-induced decreases in carbon fixation of nutrient-limited phytoplankton without a subsequent decrease in biomass implies an inconsistency in the mass balance for carbon. This carbon-budget discrepancy is not yet fully understood. However, some insight toward the explanation of this discrepancy may be provided by a physiological characteristic of marine phytoplankton, namely carbon exudation. Photosynthetic production of simple carbon compounds (photosynthates) by marine phytoplankton often exceeds their nutrient-limited rate of utilization for growth (Hellbust, 1974; Williams, 1990). The "excess" photosynthate is exuded into the surrounding medium. Decreases in carbon fixation by UVBR without a subsequent

decrease in biomass could occur if the amount of carbon incorporated into cellular components was controlled by the availability of limiting nutrient and the decrease in photosynthesis by UVBR was accounted for by a decrease in photosynthate exudation.

Decreases in photosynthate exudation by increasing surface UVBR intensities could have community level effects in nutrient-limited regions of the ocean by affecting the nutrient-recycling efficiency between phytoplankton and bacteria (Azam & Ammerman, 1984). Repression of nutrient recycling could, in turn, result in lower phytoplankton growth rates and biomass. The possible decrease in nutrient-limited phytoplankton biomass resulting from the effects of UVBR on nutrient recycling does not conflict with the concept of a competitive interaction existing between UVBR stress and nutrient limitation (Chapter 3). The nutrient recycling scenario for a UVBR induced decrease in nutrient-limited phytoplankton biomass results from a UVBR induced increase in the nutrient stress (i.e., the most limiting factor) of the system, rather than an increase in the direct effects of UVBR on the phytoplankton community.

Stratospheric ozone concentrations are decreasing at an alarming rate and require the development of predictive models for estimating the effects of enhanced UVBR on marine ecosystems. Predictive models of ozone depletion effects would provide support for international efforts to eliminate

ozone destroying chemicals. Dose-responses and action spectra for UVBR inhibition of carbon and nitrogen uptake determined from my research should be useful for modeling the effects of increased surface UVBR on marine phytoplankton. Additional research on UVBR effects should address new questions regarding the role of solar UVBR in surface photoinhibition, particularly with respect to 1) the importance of inter-specific competition, 2) the effects of vertical mixing on photoadaptation, 3) the connection between measurements on carbon uptake, growth and biomass, and 4) the influence of nutritional stress and nutrient recycling on estimates of UVBR inhibition.

BIBLIOGRAPHY

Anderson, J.G., Toohey, D.W., and Brune, W.H. 1991. Free radicals within the Antarctic vortex: The role of CFCs in Antarctic ozone loss. Science. 252:39-46.

Azam, F. and Ammerman, J.W. 1984. Cycling of organic matter by bacterioplankton in pelagic marine ecosystems: microenvironmental considerations. In: M.J.R. Fasham [ed.]. Flows of energy and materials in marine ecosystems. Plenum Press. pp. 345-360.

Behrenfeld, M.J., Hardy, J.T., and Lee II, H. 1992. Chronic effects of ultraviolet-B radiation on growth and cell volume of *Phaeodactylum tricornutum* (Bacillariophyceae). J. Phycol. 28(6): 757-760.

Behrenfeld, M.J., Hardy, J.T., Gucinski, H., Hanneman, A., Lee II, H., and Wones, A. 1993. Effects of ultraviolet-B radiation on primary production along latitudinal transects in the South Pacific Ocean. Mar. Env. Res. 35:(in press).

Bidigare, R.R. 1989. Potential effects of UV-B radiation on marine organisms of the southern ocean: Distributions of phytoplankton and krill during austral spring. Photochem. Photobiol. 50(4):469-477.

Bornman, J.F. 1989. Target sites of UV-B radiation in photosynthesis of higher plants. J. Photochem. Photobiol., B:Biol. 4:145-158.

Bothwell, M.L., Sherbot, D., Roberge, A.C., and Daley, R.J. 1993. Influence of natural ultraviolet radiation on lotic periphytic diatom community growth, biomass accrual, and species composition: Short-term versus long-term effects. J. Phycol. 29(1):24-35.

Brasseur, G. and De Rudder, A. 1983. Agents and effects of ozone trends in the atmosphere. In: R.C. Worrest and M.M. Caldwell [eds.]. Stratospheric ozone reduction, solar ultraviolet radiation and plant life. NATO Advanced Science Institutes Series, Vol. 8. Springer-Verlag Publish. Berlin, Germany. pp. 1-28.

Brune, W.H., Anderson, J.G., Toohey, D.W., Fahey, D.W., Kawa, S.R., Jones, R.L., McKenna, D.S., and Poole, L.R. 1991. The potential for ozone depletion in the Arctic polar stratosphere. Science. 252:1260-1265.

Bühlmann, B., Bossard, P., Uehlinger, U. 1987. The influence of longwave ultraviolet radiation (u.v.-A) on the photosynthetic activity (^{14}C-assimilation) of phytoplankton. J. Plankt. Res. 9(5):935-943.

Caldwell, M.M. 1971. Solar UV irradiation and the growth and development of higher plants. In: Giese A.C. [ed.]. Photophysiology, Vol. 6. Academic Press, New York. p 131.

Caldwell, M.M., Robberecht, R., and Flint, S.D. 1983. Internal filters: prospects of UV-acclimation in higher plants. Physiol. Plant. 58:445-450.

Calkins, J. and Thordardottir, T. 1980. The ecological significance of solar UV radiation on aquatic organisms. Nature 283: 563-566.

Crawford, M. 1987. Landmark ozone treaty negotiated. Science. 237:1557.

Cullen, J.J. and Lesser, M.P. 1991. Inhibition of photosynthesis by ultraviolet radiation as a function of dose and dosage rate: Results for a marine diatom. Mar. Biol. 111:183-190.

Cullen, J.J., Neale, P.J., Lesser, M.P. 1992. Biological weighting function for the inhibition of phytoplankton photosynthesis by ultraviolet radiation. Science. 258:646-650.

Davey, E.W., Gentile, J.H., Erickson, S.J., and Betzer, P. 1970. Removal of trace metals from marine culture media. Limnol. Oceanogr. 15(3):486-488.

Döhler, G. 1984a. Effect of UV-B Radiation on biomass production, pigmentation and protein content of marine diatoms. Z. Naturforsch 39(c):634-638.

Döhler, G. 1984b. Effect of UV-B Radiation on the marine diatoms *Lauderia annulata* and *Thalassiosira rotula* grown in different salinities. Mar. Biol. 83:247-253.

Döhler, G. 1987. Effect of irradiation on nitrogen metabolism in marine diatoms and phytoplankton. Océanis. 13:487-93.

Döhler, G., Worrest, R.C., Biermann, I., and Zink, J. 1987. Photosynthetic $^{14}CO_2$ fixation and [^{15}N]-ammonia assimilation during UV-B radiation of *Lithodesmium variabile*. Physiol. Plant. 70:511-515.

Döhler, G. 1988. Effect of UV-B (280-320 nm) radiation on the ^{15}N-nitrate assimilation of some algae. Plant Physiol. (Life Sci. Adv.) 7:79-84.

Ekelund, N.G.A. 1990. Effects of UV-B radiation on growth and motility of four phytoplankton species. Physiol. Plant. 78:590-594.

El-Sayed, S.Z., Stephens, F.C., Bidigare, R.R., and Ondrusek, M.E. 1990. Effect of ultraviolet radiation on Antarctic marine phytoplankton. In: K.R. Kerry and G. Hempel [eds.]. Antarctic ecosystems: Ecological change and conservation. Springer-Verlag, Berlin, Heidelberg. p. 379-385.

Falkowski, P.G. and Woodhead, A.D. 1992. Primary productivity and biogeochemical cycles in the sea. Plenum Press. New York, N.Y. 550 pp.

Fisher, R. and McKinley, E.B. 1927. The resistance of different concentrations of a bacteriophage to ultraviolet rays. J. Infect. Disea. 40(3):399-403.

Frederick, J.E. and Lubin, D. 1988. The budget of biologically active ultraviolet radiation in the earth-atmosphere system. J. Geophys. Res. 93(D4):3825-3832.

Frederick, J.E. and Snell, H. 1988. Ultraviolet radiation levels during the Antarctic spring. Science. 22:438-439.

Frederick, J.E. 1993. Ultraviolet sunlight reaching the earth's surface: A review of recent research. Photochem. Photobiol. 57(1):175-178.

Green, A.E.S, Cross, K.R., and Smith, L.A. 1980. Improved analytic characterization of ultraviolet skylight. Photochem. Photobiol. 31:59-65.

Gucinski, H., Bates, T.S., Wones, A.G., and Behrenfeld, M.J. 1990. Dimethylsulfide production: Effects of UV-B and PAR on heterogeneous phytoplankton populations. In: N.V. Blough and R.G. Zepp [eds.]. Effects of Solar Ultraviolet Radiation on Biogeochemical Dynamics in Aquatic Environments. Woods Hole Oceanog. Inst. Tech. Rept. WHOI-90-09, pp. 129-132.

Guillard, R., Ryther, J. 1962. Studies on marine planktonic diatoms I. *Cyclotella nana* (Hustedt) and *Detonula confervacae* (Cleve). Gran. Can. J. Microbiol. 8:229-239.

Hardy, J.T. and Gucinski, H. 1989. Stratospheric ozone depletion: Implications for marine ecosystems. Oceanogr. 2:18-21.

Harm, W. 1980. Biological effects of ultraviolet radiation. Cambridge University Press, Cambridge.

Helbling, E.W., Villafañe, V., Ferrario, M., and Holm-Hansen, O. 1992. Impact of natural ultraviolet radiation on rates of photosynthesis and on specific marine phytoplankton species. Mar. Ecol. Prog. Ser. 80:89-100.

Hellebust, J.A. 1974. Extracellular products. In: W.D.P. Stewart [ed.]. Algal physiology and biochemistry. Univ. California Press, Berkeley. pp. 838-863.

Hirosawa, T. and Miyachi, S. 1983. Inactivation of Hill reaction by long-wavelength ultraviolet radiation (UV-A) and its photoreactivation by visible light in the cyanobacterium, *Anacystis nidulans*. Arch. Microbiol. 135:98-102.

Hobson, L.A. and Hartley, F.A. 1983. Ultraviolet irradiance and primary production in a Vancouver Island fjord, British Columbia, Canada. J. Plankt. Res. 5(3):325-331.

Jagger, J. 1981. Near-UV radiation effects on microorganisms. Photochem. Photobiol. 34:761-768.

Jerlov, N.G. 1950. Ultraviolet radiation in the sea. Nature. 166:111-112.

Jokiel, P.L. and York, R.H. Jr. 1984. Importance of ultraviolet radiation in photoinhibition of microalgal growth. Limnol. Oceanogr. 29(1):192-199.

Jones, L. and Kok, B. 1966. Photoinhibition of chloroplast reactions: I. Kinetics and action spectra. Plant Physiol. 41:1037-1043.

Karentz, D., Cleaver, J.E., and Mitchell, D.L. 1991. Cell survival characteristics and molecular responses of Antarctic phytoplankton to ultraviolet-B radiation. J. Phycol. 27:326-341.

Kerr, R.A. 1989. Ozone hits bottom again. Science. 246:324.

Kester, D.R., Duedall, I.W., Connors, D.N., and Pytkowicz, R.M. 1967. Preparation of artificial seawater. Limnol. Oceanogr. 12(1): 176-178.

Kirk, J.T.O. 1983. Light and photosynthesis in the aquatic environment. Cambridge Univ. Press. New York, N.Y. 401 pp.

Kruger, C.H. Jr., Dickinson, R.E., Friend, J.P., Hunten, D.M., and McElroy, M.B. 1982. Causes and effects of stratospheric ozone reduction: An update. National Academy Press. Washington D.C.

Kulandaivelu, G., Maragatham, S., and Nedunchezhian. 1989. On the possible control of ultraviolet-B induced response in growth and photosynthetic activities in higher plants. Physiol. Plant. 76:398-404.

Kyle, D.J., Osmond, C.B., and Arntzen, C.J. [eds.]. 1987. Photoinhibition, Vol. 9. Elsevier Science Publish. Comp. New York, N.Y. 314 pp.

Lesser, M.P. and Shick, J.M. 1989. Effects of irradiance and ultraviolet radiation on photoadaptation in the zooxanthellae of *Aiptasia pallida*: primary production, photoinhibition, and enzymic defenses against oxygen toxicity. Mar. Biol. 102:243-255.

Liebig, J. 1840. Chemistry in its application to agriculture and physiology. Taylor and Walton Publish. London. (4th ed., 1847).

Lorenzen, C. 1979. Ultraviolet radiation and phytoplankton photosynthesis. Limnol. Oceanogr. 24(6):1117-1120.

Lubin, D., Frederick, J., Booth, C., Lucas, T., and Neuschuler, D. 1989. Measurement of enhanced springtime ultraviolet radiation at Palmer Station Antarctica. Geophys. Res. Lett. 16(8):783-785.

Lubin, D., Mitchell, B.G., Frederick, J.E., Alberts, A.D., Booth, C.R., Lucas, T., and Neuschuler, D. 1992. A contribution toward understanding the biospherical significance of Antarctic ozone depletion. J. Geophys. Res. 97(D8):7817-7828.

Lyman, H., Epstein, H.T., and Schiff, J.A. 1961. Studies of chloroplast development in *Euglena* I. Inactivation of green colony formation. Biochim. Biophys. Acta. 50:301-309.

Mantai, K.E., Wong, J., and Bishop, N.I. 1970. Comparison studies on the effects of ultraviolet irradiation on photosynthesis. Biochim. Biophys. Acta. 197:257-266.

Manzer, L.E. 1990. The CFC-Ozone issue: Progress on the development of alternatives to CFCs. Science. 249:31-35.

Martin, J.H., Gordon, R.M., and Fitzwater, S.E. 1991. The case for iron. Limnol. Oceanogr. 36(8):1793-1802.

Maske, H. 1984. Daylight ultraviolet radiation and the photoinhibition of phytoplankton carbon uptake. J. Plankt. Res. 6(2):351-357.

McElroy, M.B., and Salawitch, R.J. 1989. Changing composition of the global stratosphere. Science. 243:763-770.

McLeod, G.C. and Kanwisher, J. 1962. The quantum efficiency of photosynthesis in ultraviolet light. Physiol. Plant. 15:581-586.

Molina, M.J. and Roland, F.S. 1974. Stratospheric sink for chlorofluoromethanes - Chlorine atom catalyzed destruction of ozone. Nature. 249:810-812.

Moss, S.H. and Smith, K.C. 1981. Membrane damage can be a significant factor in the inactivation of *Escherichia coli* by near-ultraviolet radiation. Photochem. Photobiol. 33:203-210.

Murphy, T.M. 1983. Membranes as targets of ultraviolet radiation. Physiol. Plant. 58:381-388.

Murphy, T.P. 1980. Ammonium and nitrate uptake in the Lower Great Lakes. Can. J. Fish. Sci. 37:1365-1372.

Neale, P.J. 1987. Algal photoinhibition and photosynthesis in the aquatic environment. In: Kyle, D.J., Osmond, C.B., and Arntzen, C.J. [eds.]. Photoinhibition, Vol. 9. Elsevier Science Publish. Comp. New York, N.Y., 314 pp.

Paerl, H.W., Bland, P.T., Bowles, N.D., and Haibach, M.E. 1985. Adaptation to high-intensity, low-wavelength light among surface blooms of the cyanobacterium *Microcystis aeruginosa*. Appl. Environ. Microbiol. 49(5):1046-1052.

Palenik B, Price, N.M., and Morel, F.M.M. 1991. Potential effects of UV-B on the chemical environment of marine organisms: A review. Environ. Pollut. 70:117-130.

Parsons, T.R., Maita, Y., and Lalli., C.M. 1984. A manual of chemical and biological methods for seawater analysis. Pergamon Press (1st ed), Oxford, Great Britain.

Platt, T., Gallegos, C.L., and Harrison, W.G. 1980. Photoinhibition of photosynthesis in natural assemblages of marine phytoplankton. J. Mar. Res. 38(4):687-701.

Quaite, F.E., Sutherland, B.M., and Sutherland, J.C. 1992. Action spectrum for DNA damage in alfalfa lowers predicted impact of ozone depletion. Nature. 358:576-578.

Rambler, M.B. and Margulis, L. 1980. Bacterial resistance to ultraviolet irradiation under anaerobiosis: Implications for pre-phanerozoic evolution. Science. 210(7):638-640.

Rodhe. H. 1990. A comparison of the contribution of various gases to the greenhouse effect. Science. 248:1217-1219.

Schoeberl, M.R. and Hartmann, D.L. 1991. The dynamics of the stratospheric polar vortex and its relation to springtime ozone depletions. Science. 251:46-52.

Setlow, R. 1974. The wavelengths in sunlight effective in producing skin cancer: A theoretical analysis. Proc. Nat. Acad. Sci. U.S.A. 71:3363-3366.

Sigleo, A.C. and Behrenfeld, M.J. 1992. Effects of ultraviolet-B radiation on marine biogeochemical cycles. U.S. Environmental Protection Agency, Newport, Oregon. Tech. Rprt. #ERLN-N206.

Smith, R.C., Baker, K.S., Holm-Hansen, O., and Olson, R. 1980. Photoinhibition of photosynthesis in natural waters. Photochem. Photobiol. 31:585-592.

Smith, R.C. and Baker, K.S. 1981. Optical properties of the clearest natural waters (200-800 nm). Applied Optics 20(2):177-184.

Smith, R.C., Prézelin, B.B., Baker, K.S., Bidigare, R.R., Boucher, N.P., Coley, T., Karentz, D., MacIntyre, S., Matlick, H.A., Menzies, D., Ondrusek, M., Wan, Z., and Waters, K.J. 1992. Ozone depletion: Ultraviolet radiation and phytoplankton biology in Antarctic waters. Science (Wash. D.C.). 255:952-959.

Stolarski, R.S., Bloomfield, P., and McPeters, R.D. 1991. Total ozone trends deduced from Nimbus 7 TOMS data. Geophys. Res. Lett. 18(6):1015-1018.

Stolarski, R., Bojkov, R., Bishop, L., Zerefos, C., Staehelin, J., and Zawodny, J. 1992. Measured trends in stratospheric ozone. Science. 256:342-349.

Strickland, J.D.H. and T.R. Parsons. 1972. A practical handbook of seawater analysis, 2nd ed. Bull. Fish. Res. Bd. Can. 167 pp.

Strid, Å., Chow, W.S., and Anderson, J.M. 1990. Effects of supplementary ultraviolet-B radiation on photosynthesis in *Pisum sativum*. Biochimuca Biophysica Acta. 1020:260-268.

Teramura, A.H. 1980. Effects of ultraviolet-B irradiances on soybean. Physiol. Plant. 48:333-339.

Thomson, B.E., Worrest, R.C., and VanDyke, H. 1980. The growth response of an esturine diatom (*Melosira nummuloides* [Dillw.] Ag.) to UV-B (290-320 nm) radiation. Estuaries 3(1):69-72.

Trocine, R.T., Rice, J.D., and Wells, G.N. 1981. Inhibition of seagrass photosynthesis by ultraviolet-B radiation. Plant Physiol. 68:74-81.

Van Baalen, C. and O'Donnell, R. 1972. Action spectra for ultraviolet killing and photoreactivation in the blue-green alga *Agmenellum quadruplicatum*. Photochem. Photobiol. 15:269-274.

Voytek, M.A. 1990. Addressing the biological effects of decreased ozone on the Antarctic environment. Ambio. 19(2):52-61.

Watson, R.T., Kurylo, M.J., Prather, M.J., and Ormond, F.M. 1990. Present state of knowledge of the upper atmosphere 1990: An assessment report. Report to Congress. NASA Office of Space Science and Applications, Washington D.C. NASA Refer. Publ. #1242.

Wellmann, E., Schneider-Ziebert, U., and Beggs, C.J. 1984. UV-B inhibition of phytochrome-mediated anthocyanin formation in *Sinapis alba L.* cotyledons. Plant Physiol. 75:997-1000.

Williams, P.J. leB. 1990. The importance of losses during microbial growth: Commentary on the physiology, measurement and ecology of release of dissolved organic material. Mar. Microb. Food Webs. 4:175.

Winer, B.J. 1962. Statistical principles in experimental design. McGraw-Hill. New York, N.Y.

Wolniakowski, K.U. 1980. The physiological response of a marine phytoplankton species, *Dunaliella tertiolecta*, to mid-wavelength ultraviolet radiation. Masters Thesis. Oregon State University, Oregon.

Wood, W.f. 1987. Effect of solar ultra-violet radiation on the kelp *Ecklonia radiata*. Mar. Biol. 96:143-150.

Worrest, R.C., VanDyke, H., and Thomson, B.E. 1978. Impact of enhanced simulated solar ultraviolet radiation upon a marine community. Photochem. Photobiol. 27:471-478.

Worrest, R.C., Brooker, D.L., and Van Dyke, H. 1980. Results of a primary productivity study as affected by the type of glass in the culture bottles. Limnol. Oceanogr. 25(2):360-364.

Worrest, R., Wolniakowski, K.U., Scott, J., Brooker, D., Thomson, B., and Van Dyke, H. 1981a. Sensitivity of marine phytoplankton to UV-B radiation: Impact upon a model ecosystem. Photochem. Photobiol. 33:223-227.

Worrest, R.C., Thomson, B.E., and VanDyke, H. 1981b. Impact of UV-B radiation upon esturine microcosms. Photochem. Photobiol. 33:861-867.

Worrest, R.C. 1983. Impact of solar ultraviolet-B radiation (290-320 nm) upon marine microalgae. Physol. Plant. 58:428-434.

Yung, Y.L., Allen, M., Crisp, D., Zurek, R.W., and Sander, S.P. 1990. Spatial variation of ozone depletion rates in the springtime Antarctic polar vortex. Science. 248:721-724.

Zaneveld, J.R.V. 1975. Penetration of ultraviolet radiation into natural waters. In: Impacts of climatic change on the biosphere. CIAP Monograph 5, Pt. 1 - Ultraviolet radiation effects. Department of Transportation. Climatic Impact Assessment Program. DOT-TST-75-55.

Zifka, L.H., Teramura, A., and Sullivan, J. 1992. Physiological sensitivity of plants along an elevational gradient to UV-B radiation. Amer. J. Bot. 78(8):863-871.